ROTATION OF LATE CENOZOIC EXTENSIONAL STRESSES, YUCCA FLAT REGION, NEVADA TEST SITE, NEVADA

BY

HOLLY DOCKERY ANDER

Ph.D. THESIS

RICE UNIVERSITY   HOUSTON, TEXAS

MAY 1984

RICE UNIVERSITY

ROTATION OF LATE CENOZOIC EXTENSIONAL STRESSES, YUCCA FLAT REGION,
NEVADA TEST SITE, NEVADA

BY HOLLY DOCKERY ANDER

A THESIS SUBMITTED
IN PARTIAL FULFILLMENT OF THE
REQUIREMENT OF THE DEGREE

DOCTOR OF PHILOSOPHY

APPROVED, THESIS COMMITTEE

HOUSTON, TEXAS

MAY 1984

ABSTRACT

The Nevada Test Site (NTS) is located in the southern Basin and Range where the geology is typified by complexly deformed Paleozoic sedimentary rocks underlying Tertiary and Quaternary volcanics and alluvium all displaced by Cenozoic normal faults. The purpose of this study is to interpret the history of change in Cenozoic extensional stress orientations using ash-flow tuff distributions, surface fault configurations, and slickenside analyses.

Extensive drill hole data collected from Yucca Flat within NTS were used to construct isopach and structure contour maps of Cenozoic units occupying the northerly-trending basin. The configuration of these units indicates that the north-south-trending faults controlling present day basin morphology were inactive during deposition of the volcanic rocks from approximately 25 to 11 myBP. However, after 11 myBP, the overlying sedimentary sequence was strongly influenced by these faults and consequent basin development. In particular, an inordinately thick section of late Tertiary and Quaternary alluvium occurs at the southwestern end of Yucca Flat.

Southwest-striking faults at the southwestern of Yucca Flat are postulated to be deflected at their northeast ends, becoming continuous with the north-south basin forming fault sets. The northeast faults exhibit predominantly left-lateral displacement occurring post-11 myBP. This sense of motion is incompatibile with the N50°W extension determined today via _in situ_ measurements. The north-south faults are primarily dip-slip with a small component of right-lateral motion. The

thick sedimentary section found in southern Yucca Flat at the inter-section of the southwest-striking and north-south-striking faults formed as a pull-apart basin which developed syndepositionally with the alluvium. Observed offsets of volcanic units by the southwesterly striking faults as well as slickenside analyses of data from the major fault zones throughout the area indicates a N78°W extension operating since 11 myBP. After formation of much of the Yucca Flat basin, the least principal stress rotated to N50°W. This rotation apparently occurred very recently and the new stress orientation has had little effect on the fault patterns or fault displacements of the area.

Synthesis of this work with other studies throughout the southern Basin and Range show a consistant clockwise rotation of least principal stress through an angle of 90° in the past 17 my.

Acknowledgments

I would like to thank my major advisor, John Oldow, for supplying the initial ideas for this topic, for numerous helpful discussions in the course of the study, and for revising the final copy of this manuscript. Frank Byers also provided many hours of discussion, his extensive knowledge of the NTS region proved invaluable. H.G. Ave Lallemant and Mark Ander made suggestions which were incorporated into the paper. Paul Orkild, Will Carr, and Bob Scott of the USGS in Denver as well as Nancy Marusak, Don Krier, Rick Warren, and Ward Hawkins of Los Alamos have at various times shared their knowledge of Test Site geology as well. Mary Lou Zoback provided a revised copy of the Angelier slickenside analysis program which was used in the course of the study. Jack House and Wes Myers worked to provide financial support for this project. Barbara Hahn typed the manuscript and Mary Ann Olson and Luween Smith drafted the plates showing the isopachs and structure contours and several of the illustrations.

Finally, I would like to thank my mother and father, Kenneth and Anabel Dockery, and my husband, Mark Ander for supplying moral support for the duration.

Table of Contents

List of Figures

List of Tables

List of Plates

(Located in back cover)

List of Plates

(Located in back cover)

INTRODUCTION

As more and more data concerning the Cenozoic history of the Basin and Range Province (Figure 1) is gathered, interpretation of the tectonic development of the region presents an increasingly complex picture. The pervasive north-northeast-trending structural grain of the Great Basin subprovince of the Basin and Range led earlier workers to infer that a single least-principal stress, oriented west-northwest, controlled extensional faulting since its inception in the mid-Cenozoic (Hamilton and Myers, 1966; McKee et al., 1970). Recent studies have recognized the existence of pre-existing Cenozoic extensional fault systems which are obscured by the overpowering north-northeast structural grain of the region (Zoback and Thompson, 1978; Burke and McKee, 1979; Oldow et al., 1980). Although the current west-northwest to westerly extension direction has been involved to produce movement on faults throughout the Cenozoic time in the Basin and Range (Wright, 1976; Speed and Cogbill, 1979; Zoback and Zoback, 1980; Miller et al., 1983); there is an increasing body of evidence supporting a secular variation in the orientation of least-principal stress resulting in changes in regional fault patterns and displacement histories (Anderson and Ekren, 1977; Zoback and Thompson, 1978; Oldow et al., 1980; Dockery, 1982).

North-northeasterly faults became the dominant extensional structures sometime after 13-10 myBP (Zoback et al., 1981; Stewart, 1982). Movement on older faults of various orientations were probably initiated as long ago as 35 myBP (Eaton, 1982) to 36 myBP (Stewart,
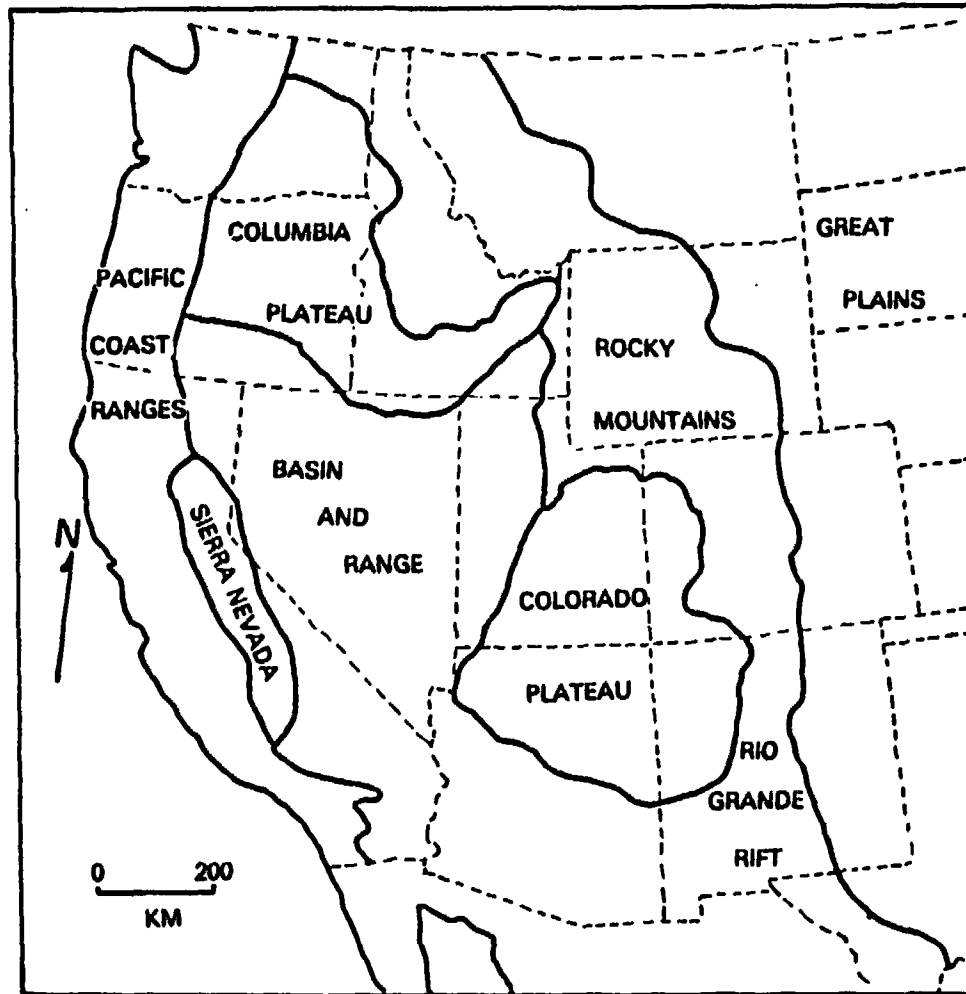
Figure 1. Boundaries of major physiographic provinces of the western United States.

1982). Extension on these older fault sets occurred in a convergent plate boundary setting with subduction of the Farallon plate beneath North America.

Several models, evolving over the last decade, have focused on particular aspects of the tectonic development of the Great Basin and to a lesser degree the Basin and Range as a whole. Atwater (1970) proposed a model whereby Basin and Range extension was a direct response to right-lateral motion occurring on the San Andreas fault system, which began as the East Pacific rise and West Coast trench collided and transform motion started between the Pacific and North American plates. Scholz et al. (1971) pointed out that Atwater's model by itself was unsatisfactory for several reasons: (1) even though the lateral components of movement could be explained by the applied shear stress, the greater amount of extension due to normal faulting was not; (2) the Atwater model predicted tectonism should be more intense in the western Great Basin, dying out to the east; a configuration not observed seismically or in the volcanic history, and (3) that high regional heat flow could not be explained by the simple shear model. An additional point not mentioned by Scholz et al. (1971) is that the timing of the extensional history is not adequately explained by the model. Atwater's model calls for the initial contact of the Pacific and North American plates to occur at about 29 myBP. It is reasonable to expect that some critical length of transform fault is necessary to induce right-lateral shear over such a large area as the Basin and Range. It is readily apparent then that the first stages of extension which occurred at about 36 myBP (Eaton, 1982) cannot be accounted for

by the Atwater model. Scholz et al. (1971) proposed that the change in the plate boundary geometry gave rise to a relaxation of compressive stress allowing an upwelling of a mantle diapir derived from melting of the subducted lithospheric slab. The diapiric upwelling was the proposed source of extensional stress upon which a right-lateral shear from the San Andreas fault was then superimposed. Neither the models of Atwater (1970) nor Scholz et al. (1971) fully account for the presence of earlier (pre 13 myBP) extension features found widely dispersed throughout the Basin and Range. Cross and Pilger (1978) explained the early extensional history in terms of changes in absolute plate velocities. They speculated that a decreased convergence rate between the North American and Farallon plates allowed relaxation in the back arc, resulting in regional extensional. Although this process may have been operating to produce extension, the timing (post 20 myBP) deduced by Cross and Pilger does not explain the oldest extensional patterns.

Eaton (1984) recognized the timing problem and presented a model for extension in the Basin and Range in which intra-arc spreading followed by back-arc spreading gives way to transform-related oblique extension. He envisions the earliest stage, occurring during subduction of the Farallon plate (~37 myBP), as typified by low-angle listric normal faults and associated widespread calc-alkaline volcanism in the upper plate. During this interval, the rate of plate convergence dropped dramatically but the azimuth of relative plate motion convergence was essentially constant (Eaton, 1982). This slowing of plate motion was inferred to produce a weakening of the plate-plate

couple, whereby upper plate extension was allowable by relaxation of the overriding plate. It also is expected that the azimuth of the resulting extension direction would be similar to that of the preceding compression, and indeed both of these strain fields were oriented approximately west-southwest (Eaton, 1982). The change from intra-arc to back-arc spreading at around 22-18 myBP and is recognized on the basis of the change from an area of diffuse, widespread volcanic centers to the formation of a narrow and well-defined calc-alkaline volcanic arc. The mechanism causing the change is not understood. Plate convergence rates do not show a radical change as observed at the initiation of intra-arc extension (Eaton, 1984). Also, the theory of a progressively steepening subducting slab and resulting constriction of the arc (Coney and Reynolds, 1977) does not seem possible from the extreme rapidity of steepening required by current data interpretation (Eaton, 1984). However, extension continued in the same orientation. After the formation of the transform boundary, Eaton (1984) proposes that at some critical point the extension direction was abruptly affected by the transform motion and rotated clockwise into its present northwesterly direction approximately 10 myBP.

In a recent paper, Ingersoll (1982) proposed that the geometry of the Mendocino triple junction produced a tectonic instability allowing internal extensional deformation of the North American plate after 30 myBP in areas where earlier tectonic events had weakened the crust. Both the models of Eaton (1982) and Ingersoll (1982) require clockwise rotations of least principal stress orientation after the initiation of extension. Studies of the remnant paleomagnetic field of Tertiary

volcanic rocks in the western Cordillera and Pacific Coast (Magill and Cox, 1981) and detailed studies of fault movements (summarized in Zoback et al., 1981) support systematic clockwise rotation of the extensional stress from west-southwest to west-northwest through time.

This study, focuses on the secular variation of extensional stress at the Nevada Test Site (NTS) of southern Nevada (Figure 2). The data base for this investigation incorporates surface fault patterns and displacement histories, subsurface basin geometry of the Tertiary basin beneath Yucca Flat derived from extensive drillhole data, and slickenside analyses of lineations on variably oriented faults. The data are modeled and compared to current theories for plate interactions.

ELKO
•

NEVADA

RENO
•

ELY
•

TONOPAH
•

NEVADA
TEST SITE
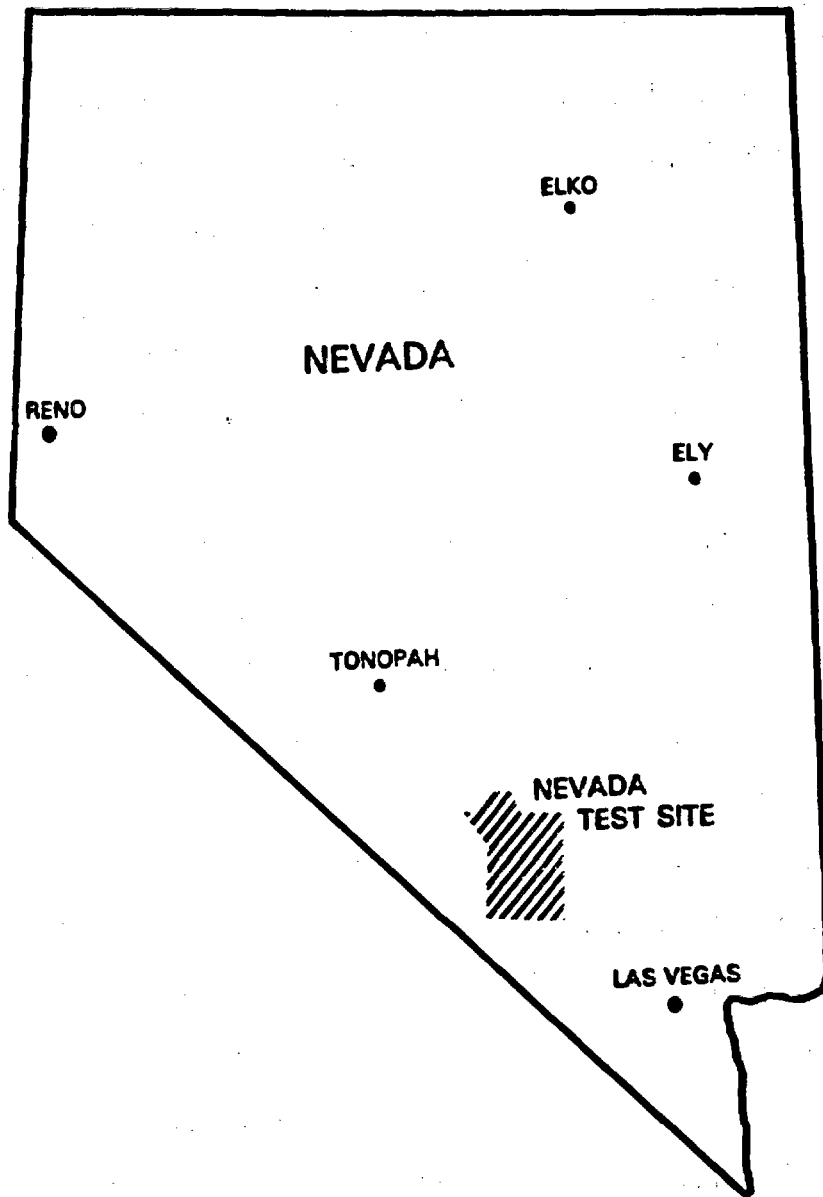
LAS VEGAS
•

Figure 2.   Location of the Nevada Test Site.

FAULTING IN SOUTHERN NEVADA

Paralleling the California-Nevada border from Las Vegas to Pyramid Lake, the northwesterly trending Walker Lane (Figure 3) disrupts the north-northeasterly linear grain of the Basin and Range. First recognized by merit of its physiographic character, the Walker Lane has been theorized to be a zone of extensive right-lateral shear. Stewart (1967) proposed 50 km of right-lateral movement on the Las Vegas shear zone at the southern end of the Walker Lane on the basis of clockwise bends and offset of Paleozoic facies markers thought to have been linear prior to Cenozoic tectonism. Further studies of the Las Vegas shear zone has led to estimates of 65 km (Longwell, 1974) to 72 km (Fleck, 1970) of right-lateral displacement. Recent paleomagnetic work (Nelson, 1983) does not support earlier interpretations and suggests that bending of the units is $\sim 20°-30°$ less than that indicated by outcrop patterns. The magnitude of shearing thus is apparently significantly decreased. The age of motion on the Las Vegas shear zone has been suggested as starting at around 17 to 15 myBP and ending at approximately 11 myBP (Fleck, 1970; Longwell, 1974).

Along the Walker Lane, 325 km northwest of Las Vegas, Albers (1967) proposed the existence of a major oroclinal bend in regional structures, stratigraphic problems, and present day topography caused by Jurassic to Cenozoic tectonism. Subsequent paleomagnetic studies of Mesozoic plutons do not support the oroclinal model because no rotation is observed (Oldow and Geissman, 1982; Callian and Geissman, 1982). The "orocline" subparallels the Precambrian to early Paleozoic
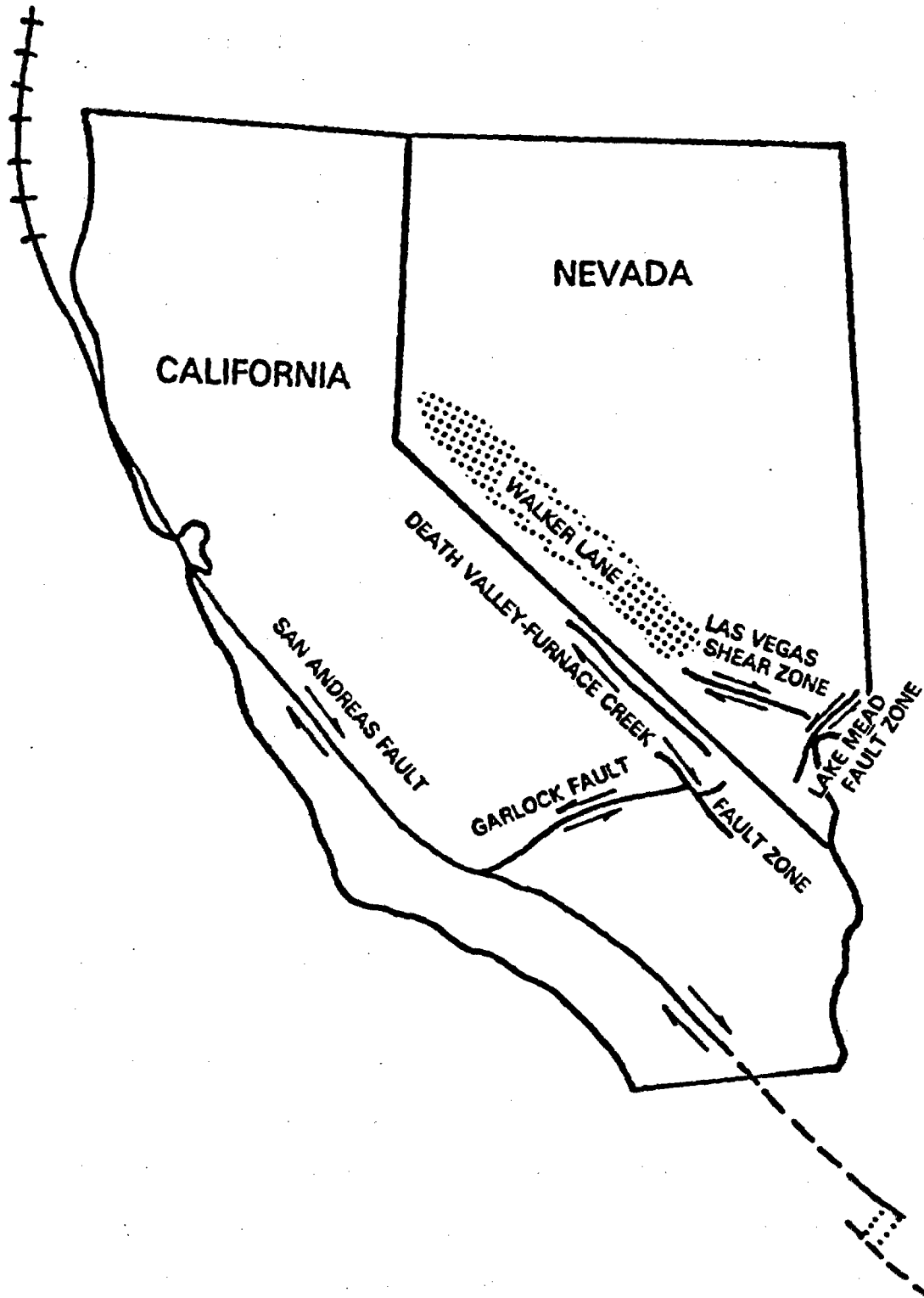
Figure 3. Fault zones in the vicinity of NTS where major lateral movement has occurred or is proposed.

continental margin deduced from strontium isotope data and from facies pattern (Oldow, 1984). Recent work on Mesozoic structures of the Roberts Mountain thrust indicate that the bend predates the Antler orogeny and is interpreted as an original curve in the continental margin (Oldow,1984). Although the evidence refutes major shearing as the cause of the nonlinearity of structural and stratigraphic patterns, studies of Tertiary fault relations do show the presence of right-lateral motion on northwest-trending faults in this region (Hardyman, 1978; Ekren et al., 1980; Oldow et al., 1980). The component of strike-slip motion on many of these faults is the result of displace-ment on faults oriented obliquely to a uniform extension direction. However a narrow zone of left-stepping en echelon right-lateral faults are recognized to have right-lateral motion in excess of that expected for faults of corresponding orientation in a field of uniform extension (Oldow et al., 1980).

Elsewhere, left-lateral faults are recognized. The Lake Mead fault zone is a northeast-trending zone of major left-lateral faults which changes its orientation to a more northerly orientation at its southern end (Figure 3). Geologic mapping south of the Lake Mead fault zone shows no southerly extension of the Las Vegas shear zone beyond its intersection with the Lake Mead fault zone (Bohannon, 1979). Approximately 65 km of left slip motion is reported for the Lake Mead fault zone (Bohannon, 1979), the majority of which occurred between 15 and 10 myBP. Studies of fault strain and patterns of movement south of Lake Mead indicate a N70°E least principal stress operating during most of this time interval; however, after about 11 to 5 myBP the extension

direction rotated to east-west (Anderson, 1982). Anderson et al. (1982) postulate that the timing and movement along both the Las Vegas shear zone and the Lake Mead fault zone argues that the two fault zones are genetically related.

If the Lake Mead fault zone and Las Vegas shear zone are conjugate shears, the bisector of the obtuse angle formed by the projected intersection (which would be the approximate orientation of the tensile stress) yields an orientation of approximately north-south. In light of the recent work which indicates an extension direction of N70°E during the time in which both zones are interpreted as active (Anderson, 1982) it is difficult to reconcile with the north-south extension. In fact, the north-south extension suggested by the con-jugate model would yield a sense of lateral offset reversed from that observed for the two fault zones. Therefore it is hard to argue for a cogenetic origin of the two fault sets as conjugate shears. Given a trend of ~N55°W for the Las Vegas shear zone and of ~N50°E for the Lake Mead fault zone, it is very easy to induce strike-slip motion on the latter in a N70°E extension field, but quite difficult on the former. Although some element of right-lateral motion should be imparted to the Las Vegas shear zone during N70°E extension, there should be an even larger component of dip-slip displacment. Based on these relations, it seems unlikely that the Las Vegas shear zone and Lake Mead fault zone were formed as conjugate shears in the stress regime active from 15-10 myBP, or that the large amount of right-lateral motion proposed for the Las Vegas shear zone could have actually occurred during this time. It is apparent that more work is required to determine what displacements

have actually occurred on the Las Vegas shear zone in this time frame and how they relate to the extensional history of the surrounding region. Of particular interest would be studies in the area northeast of Frenchman Mountain (Figure 4) where the proposed lateral motion on the two fault sets should converge in an area of extreme compression. Also, more work on the clockwise rotation of Paleozoic facies by paleo-magnetic studies is necessary to determine how much of the bend in units and faults northeast of Las Vegas Valley is due to shearing and how much may actually be the result of a primary curve formed during deposition of the units and/or Mesozoic deformation.

Basin and range style normal faults north of NTS in the Kawich and Belted Ranges have been studied by Ekren et al. (1968). They report the existence of two fault systems, the oldest of which is composed of coeval northwest and a northeast-striking faults. The age of initial movement on this fault set is placed at 26.5 myBP (penecontemporaneous with earliest tuff deposition) and is based on the observation that there were no fewer fractures observed in the Tertiary section than in the Paleozoic rocks. The northwest and northeast faults were succeeded by a north-south set which formed between 17 and 14 myBP. Significant movement on this fault set is not thought to have occurred until post-11 myBP. Age of movement was inferred by the occurrence of a rhyolite apparently extruded along north-south fractures and thought to be between 17-14 my old. There are several problems with their inter-pretations. First, many of the faults comprising the early fault set are almost east-west in orientation and may actually form an additional set which corresponds to an Oligocene extension direction described

Figure 4.   Major topographic features of southern Nevada as defined by the dashed line on the figure inset in the lower left-hand corner. Major roads in and around NTS are also shown.

later. Also, to have apparent conjugate sets active as dip-slip faults
at the same time is not possible. Therefore the timing of movement may
be questionable. Recent studies have also shown that previous correla-
tions of some rhyolites mapped at NTS are suspect (Rick Warren, pers.
comm., 1984) further complicating the use of this analysis. Finally,
mapping to the south on Yucca Mountain, discussed later, shows that
numerous north-south faults were primarily active before 11 myBP. It
is therefore difficult to determine which conclusions from Ekren et al.
(1968) are valid in light of current data. Wright (1976; 1977) pre-
sented evidence for north-south and north-northeasterly faults south-
west of NTS indicating a west-northwest extension direction with dis-
placements occurring for the most part since 3 to 4 myBP. In this same
area, north-northwesterly faults were also reported. Although these
faults were primarily associated with pre-existing features and are
less reliable as stress indicators, Wright states that there is
evidence that these faults were activated prior to the intramontane
northeasterly faults even though he interprets their extension direc-
tion to be the same as the later faults. Earlier studies performed in
the vicinity of NTS obviously do not provide a clear picture of the
actual history of Cenozoic fault movement.

PALEOZOIC AND MESOZOIC

Paleozoic rocks underlie the Cenozoic basins and outcrop in the surrounding ranges (Table 1). Ordovician, Silurian, and Lower Devonian rocks present in the NTS area consist of limestones, dolomites, shales, and quartzites representing sedimentation on a subsiding continental margin (Ross, 1977; Stewart, 1972). The developing Antler orogenic belt shed sediments into a subsiding foreland basin during uppermost Devonian and lowermost Mississippian producing a carbonate-detrital belt of shales, siltstones, sandstones, cherty-pebble conglomerate and limestones (Poole and Sandbert, 1977; Poole et al., 1977). Decrease in relief on the Antler belt caused a retreat of coarse clastics and resumption of deposition of limestones, siltstones, and sandstones in a subsiding continental shelf during the Pennsylvanian and Permian (Rich, 1977).

Major regional contraction occurred in the Jura-Cretaceous (Allmendinger and Jordan, 1981) during formation of the Sevier fold-thrust belt. Although age constraints are inadequate at NTS extensive contractional structures probably relate to this deformational event.

Several late Mesozoic quartz monzonite and granodiorite intrusions are found at NTS and have been fission-track dated at 91-101 myBP (Naeser and Maldonado, 1980). They are volumetrically small and are probably related to emplacement of the Sierra Nevada batholith approximately 100 myBP (Naeser and Maldonado, 1981).

TABLE 1

PRE-CENOZOIC ROCKS EXPOSED IN AND NEAR YUCCA FLAT, NEVADA TEST SITE
(modified from Orkild, 1982)

Age	Formation	Approximate Thickness m	Dominant Lithology (m)	
Permian (?) and Pennsylvanian	Tippipah Limestone	1100	limestone	Upper carbonate (1100)
Mississippian and Devonian	Eleana Formation	2320	argillite, quartzite	Upper clastic (2320)
Devonian	Devils Gate Limestone	420	limestone	
	Nevada Formation	465	dolomite	
Devonian and Silurian	Dolomite of Spotted Range	430	dolomite	
Ordovician	Ely Springs Dolomite	93	dolomite	Lower carbonate (4700)
	Eureka Quartzite	104	quartzite	
	Antelope Valley Limestone	466	limestone	
	Ninemile Formation	102	siltstone	
	Goodwin Limestone	290	limestone	
Cambrian	Nopah Formation	565	limestone, dolomite	
	Dunderberg Shale Member	49	shale	
	Bonanza King Formation	1400	limestone, dolomite	
	Carrara Formation	305	limestone	
		305	siltstone	
	Zabriskie Quartzite	67	quartzite	Lower clastic (2900)
	Wood Canyon Formation	695	quartzite, siltstone	
	Stirling Quartzite	915	quartzite	
Precambrian	Johnnie Formation (base not exposed)	915	quartzite, limestone, dolomite	
TOTAL THICKNESS		11,000 +		

CENOZOIC

The Cenozoic section is dominated by silicic volcanic units of mid-Tertiary age (Table 2) and sediments and basaltic lavas of late Tertiary and Quaternary age. Intensive studies of the volcanic history of NTS performed by the U.S.G.S. (e.g., Lipman et al., 1966; Noble et al., 1968, Byers et al., 1976a,b) have established a complex stratigraphic sequence of ash flows, ash falls, and bedded tuff units. Recognition of the various units and their respective distribution is a prerequisite for deciphering the structural evolution of Yucca Flat basin.

The Timber Mountain - Oasis Valley caldera complex, located in northwestern NTS (Figure 5), consists of approximately 11,000 km^2 of calc-alkalic, peralkaline, and alkali-calcic ash-flow tuffs and related rocks with ages from 16 to 9.5 myBP (Byers et al., 1976; Christiansen et al., 1977). The complex shows several cycles of resurgence which were manifested primarily as ring calderas (Byers et al., 1976). R. Warren (pers. comm., 1984) has observed from drill hole data collected on the edge of Silent Canyon Caldera that northerly faults have dictated the distribution and thickness of units ranging in age from 12.5 - 13.5 myBP. These faults have at least 250 meters of displacement in 12.5 - 13.5 myBP tuffs but offset decreases dramatically to about 30 meters in the overlying tuffs ranging in age from 11.1 - 9 myBP. There is also evidence that these faults may provide planes of weakness forming fissure vents which Warren envisions as rifts on the flank of the caldera. The majority of the Tertiary volcanic units filling Yucca Flat emanated from the Timber Mountain caldera complex.

TABLE 2

PRINCIPAL CENOZOIC VOLCANIC AND SEDIMENTARY UNITS
(modified from Orkild, 1982 and Carr, Byers, and Urkild, in press)

FORMATION, Member	Inferred Volcanic Center	General Composition	Approximate Age (m.y.)
YOUNGER BASALTS	NUMEROUS	Basalt (hawaiite)	0.3-7
THIRSTY CANYON TUFF	BLACK MOUNTAIN CALDERA	Trachytic soda rhyolite	7-9
RHYOLITE OF SHOSHONE MOUNTAIN	SHOSHONE MOUNTAIN	High-silica rhyolite	9
BASALT OF SKULL MOUNTAIN, ENAD	JACKASS FLAT(?)	Quartz-bearing basaltic andesite	10
TIMBER MOUNTAIN TUFF Intracaldera ash-flow tuffs Ammonia Tanks Member Rainier Mesa Member	TIMBER MOUNTAIN CALDERA	Rhyolite to quartz latite	10-12
PAINTBRUSH TUFF Intracaldera ash-flow tuffs Tiva Canyon Member Yucca Mountain Member Pah Canyon Member Topopah Spring Member	CLAIM CANYON CALDERA	Rhyolite to quartz latite	12-13
WAHMONIE AND SALYER FORMATIONS	WAHMONIE-SALYER CENTER	Dacitic tuffs and lavas	13-13.5
CRATER FLAT TUFF (coeval with tuffs of Area 20) Prow Pass Member Bullfrog Member Tram Member	CRATER FLAT(?). Calderas buried under basalt and alluvium	Rhyolite	13.5-14
STOCKADE WASH TUFF (coeval with Crater Flat Tuff)	SILENT CANYON CALDERA	Rhyolite	14
BELTED RANGE TUFF Grouse Canyon Member Tub Spring Member	SILENT CANYON CALDERA	Peralkaline Rhyolite	14-15
TUFF OF YUCCA FLAT	UNCERTAIN	Rhyolite	15
REDROCK VALLEY TUFF	UNCERTAIN	Rhyolite	16
FRACTION TUFF	CATHEDRAL RIDGE CALDERA	Rhyolite	17
ROCKS OF PAVITS SPRING (underlies Crater Flat Tuff)	DISPERSED	Tuffaceous sediments	14-?
HORSE SPRING FORMATION	DISPERSED	Mostly sediments	30

BLACK MOUNTAIN
CALDERA

TOLICHA PEAK ▲

SILENT CANYON
CALDERA

OAK SPRING
BUTTE

SLEEPING BUTTE
CALDERA
SEGMENT

US 95

TIMBER

MOUNTAIN

TIMBER
MOUNTAIN

CALDERA

OASIS VALLEY
CALDERA SEGMENT

TIPPIPAH
POINT

N

BEATTY

TRAM

CALDERA

CLAIM CANYON
CALDERA SEGMENT

US 95

PROW PASS AND
BULLFROG CALDERA

0	10	20 MILES
0	10	20 KILOMETERS

OUTER LIMIT OF TIMBER
MOUNTAIN-SILENT CANYON
CALDERA COMPLEX.
DASHED WHERE INDEFINITE.

PERIPHERY OF TIMBER MOUNTAIN
RESURGENT DOME.

Figure 5.   Diagram showing major volcanic centers forming the Timber
Mountain-Oasis Valley Caldera complex.   Topographic points
shown on this diagram may be located on Figure 4.

The source area for many of the "older tuffs" (~14 - ~25 myBP) found at the base of the Cenozoic section in Yucca Flat may be coincident with the Timber Mountain caldera complex as well. However, the younger Timber Mountain caldera structure and volcanic units obscure any older structures that might exist (Warren, 1983). Hence the source area of the tuffs ranging in age from 15 - ~30 myBP is not presently known. The Wahmonie-Salyar sequence (Table 2) of tuffs and lava breccias (13 - 13.5 myBP) apparently issued from the Wahmonie-Salyer volcanic center located beneath the western portion of Jackass Flats (southwest of Yucca Flat, Plate I).

Basalts covering a wide range of ages and compositions were extruded in this region. Crowe and Carr (1980) describe three episodes of basaltic volcanism related to specific tectonic settings. The oldest basalts range in age from >12 to 8.4 myBP and are closely associated with major silicic pyroclastic centers as part of a bimodal suite. The second is an episode of basalts occurring along normal faults with vp;camoc activity ranging in age from 9.1 to 6.3 myBP. Finally, a younger sequence, which was erupted after a significant hiatus in volcanic activity, is postulated to be related to a transition from extensional faulting to strike-slip motion. The younger basalts range in age from 3.7-0.3 myBP and are primarily manifested as a north-northeast-trending belt of cinder cones and volcanic fields found in Crater Flat (Figure 2) on the western border of NTS (Vaniman et al., 1982). The primary composition of the basalts of all three settings is hawaiite with subordinate amounts of alkaline basalts, tholeiite basalts, and basaltic andesites (Vaniman et al., in

review). The basalts found buried on the southwestern side of Yucca Flat have not been extensively analyzed but are probably basaltic andesites associated with the silicic episode (D. Vaniman, pers. comm., 1983).

A Tertiary volcanic-free corridor extends from the Rock Valley fault in southwestern NTS approximately 215 km south almost to Lake Mead and from the Nevada - California border northeast approximately 325 km to the southern tip of the Meadow Valley Mountains at the southeastern edge of Nevada. Eaton (1982) has suggested that this corridor forms the boundary between styles of extension in the northern and southern Basin and Range. It is interesting to note that the boundary of this "magmatic gap" to the north is approximately coincident with the left-lateral Rock Valley and Pahranaghat faults zones and to the south with the Lake Mead fault zone, also left-lateral in nature. The Cenozoic faulting found in this area is not atypical of the surrounding Basin and Range. However, the complete lack of volcanism in this area may suggest a difference in crustal thickness and or composition. Further work is necessary to determine if the crust underlying this area is indeed similar to that underlying the Basin and Range Province, or if perhaps it bears greater affinity for an adjacent terrane such as the Colorado Plateau. In such a case, the northeast trending left-lateral fault zones may be planes of weakness between areas of fundamental crustal change.

The Tertiary and Quaternary sedimentary deposits are typical of those found in arid regions with marked elevation changes. Material derived from upthrown blocks form large, coalescing colluvial fans

filling the basin. Ages of the surficial fans are Pleistocene to Recent (Fernald et al., 1968). Deeply dissected pediments are older, probably late Tertiary to early Quaternary (Fernald et al., 1968). Lenticular eolian sand deposits are also found at intervals in the alluvial section, especially in southeastern and east-central Yucca Flat (Drellack et al., 1983).

FAULTING AT NTS

OVERVIEW

Three prominent fault trends are observed at NTS, northeast, north-south, and northwest.   Short trace length faults of various orientations are also present.

The north-south faults are the present-day basin formers.   The axis of Yucca Flat trends north-south and is bounded to the east by the Jangle Ridge-Paiute Ridge fault system and to the west by the Carpetbag and related faults (Figure 6).   Most of the present-day activity in the basin occurs along the Yucca Fault (Figure 6) which runs down the center of the valley and has a map trace of 25 km.

Major northeast trending faults include the Mine Mountain (map trace ~20 km), the Cane Spring (map trace ~25 km), and the Rock Valley (map trace ~25 km) (Figure 6).   The eastern portions of the Cane Spring and the Mine Mountain faults appear to swing to the north becomming continuous with the north-south fault systems forming Yucca Flat. There is no evidence that these northeast-trending faults continue across or were offset by the north-south faults.   For this reason it is proposed that the northeast and north-south faults are part of one system (Figure 7).   In the schematic diagram, the Yucca fault is shown to be continous with the Mine Mountain fault; however, from map patterns it is not clear which northeast fault it joins.   The Rock Valley Fault does not appear to change its trend and is not detected east of Frenchman Flat in the ranges with continuous exposures of Paleozoic rocks.

1. YUCCA FAULT

2. JANGLE RIDGE/PAIUTE RIDGE FAULT SYSTEM

3. MINE MOUNTAIN FAULT SYSTEM

4. CANE SPRING FAULT SYSTEM

5. ROCK VALLEY FAULT

6. CARPETBAG FAULT

QUATERNARY ALLUVIUM

TERTIARY VOLCANICS

PRE-TERTIARY ROCKS
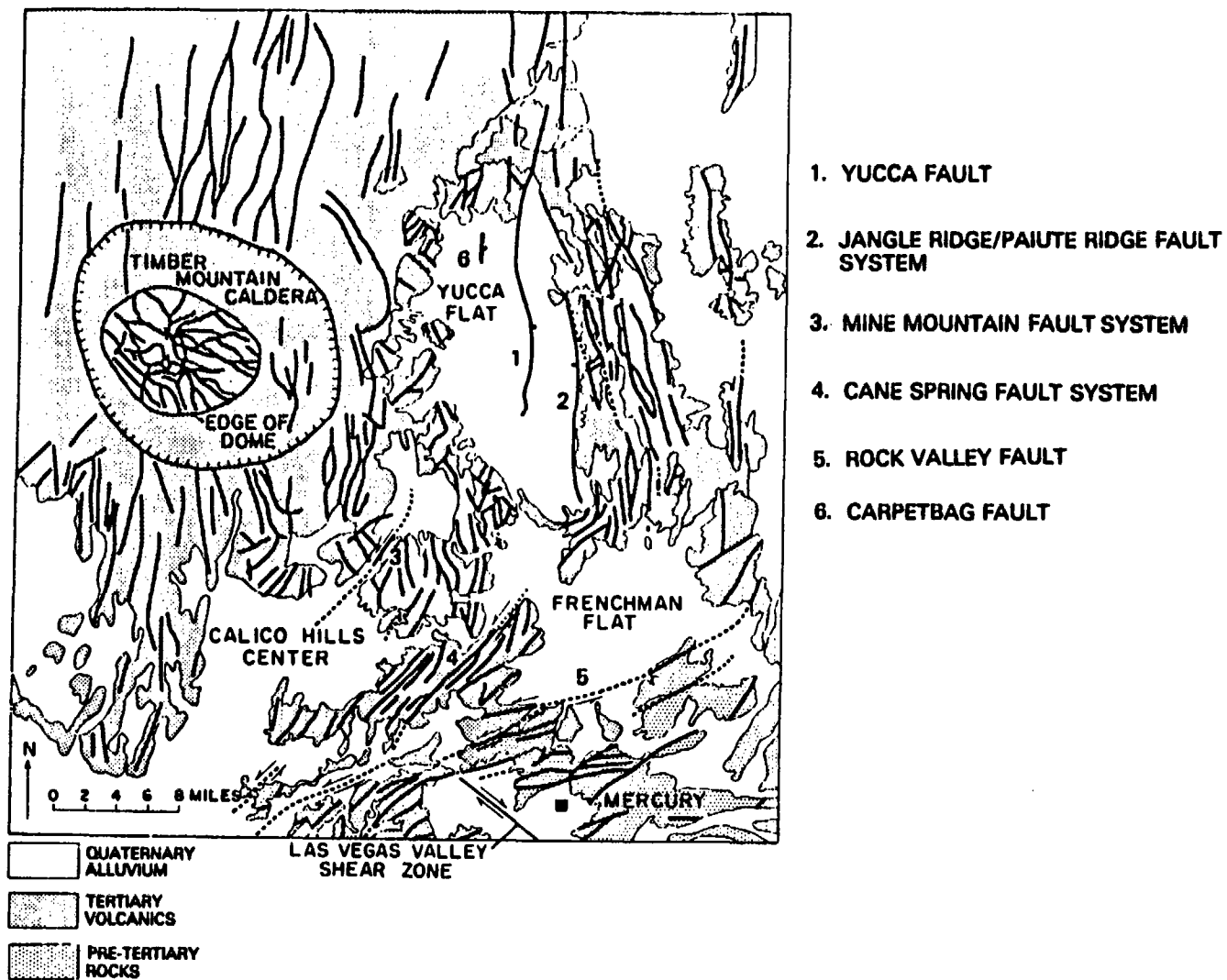
Figure 6.   Map showing major fault patterns in the vicinity of Yucca Flat.
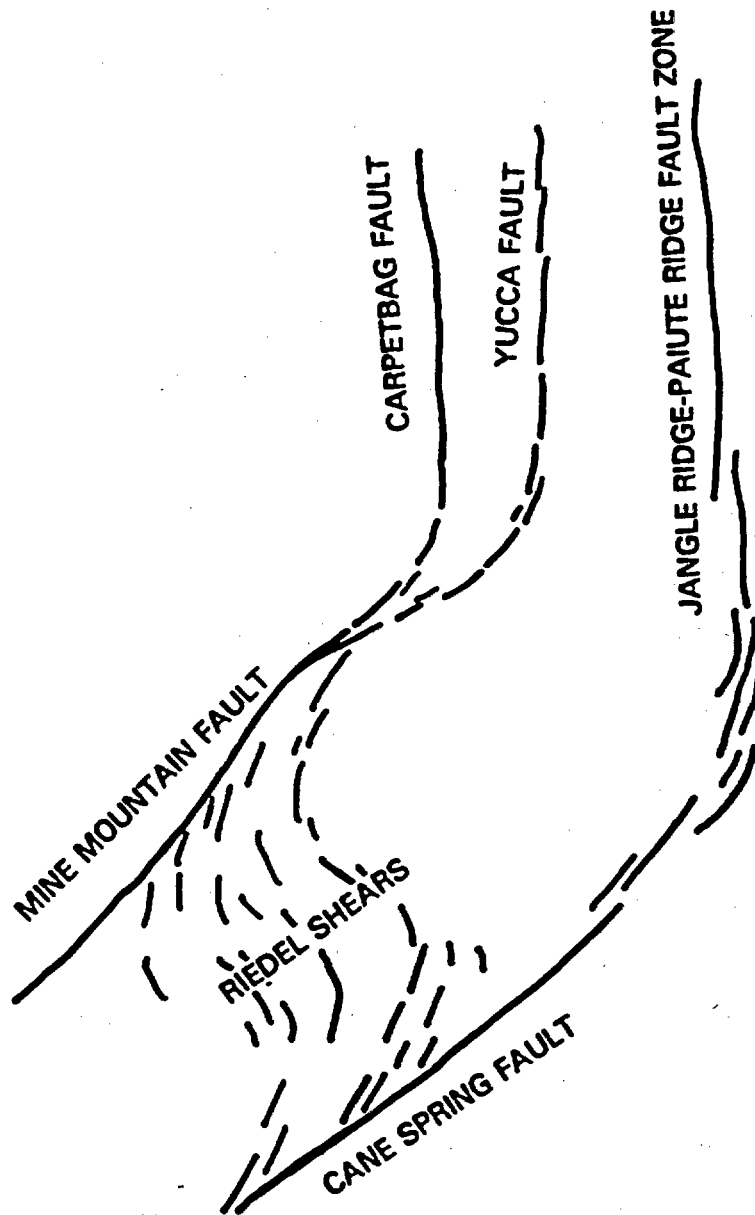
Figure 7. Schematic diagram of proposed fault interactions in the vicinity of Yucca Flat.

Northwesterly-trending faults are observed in the ranges and they are also suggested to exist in the basin through borehole geology and gravity measurements, primarily taken in conjunction with site characterization for individual nuclear tests. A large northwest-trending gravity high found bisecting the basin (Carr, 1974; Ferguson, 1981) may be related to this fault set. No Quaternary faults of this orientation have been found. The age of initiation of these faults is thought to be the same as the northeast-trending faults (Ekren et al., 1968).

Faults of short trace length with various orientations are found throughout the area. Such faults are contained in blocks bordered by major faults and probably are the result of older fault patterns as well as a locally altered stress field controlled by the large block bounding faults.

NORTH-SOUTH FAULTS

The Jangle Ridge-Paiute Ridge fault system is characterized by a series of closely-spaced faults that displace Paleozoic rocks by as much as about 60 meters in the range east of Yucca Flat (Plate I). Cenozoic vertical displacement across these faults is difficult to calculate because the volcanics they cut are extensively altered and virtually unrecognizable. However, the closely spaced, numerous fractures seem to imply a series of relatively small Cenozoic displacement faults stepping westward into the Yucca Flat basin or highly fractured blocks between large displacement faults.

The Yucca Fault traverses the length of Yucca basin as a series of left-stepping scarps - many of which have been reactivated during

nearby underground nuclear tests. Approximately 200-250 m of vertical displacement, down to the east, is found on the Yucca fault. Evidence for offset and timing of movement is shown in a subsequent chapter. Studies of the Butte fault (Plate I), a northward continuation of the Yucca fault demonstrates that dip-slip offset of the underlying Paleozoic rocks is much greater than that in the overlying Tertiary volcanics (Orkild et al., 1983), which demonstrates that a major north-south trending fault has a history of displacement before 17-20 myBP.

To the west is the Carpetbag fault system, also downdropped to the east. Over 300 meters of vertical movement on the northern part of the fault are observed and the vertical offset may increase southward. The surface expression of the Carpetbag fault formed in response to the Carpetbag nuclear detonation in 1970. Since that time, up to 6 meters of dip-slip and 0.9 meters of right-lateral movement induced by underground tests have been measured on the fault (Ander et al., in press). Gravity and seismic data extend the fault to the south (Allen Cogbill, pers. comm., 1983), a relationship confirmed by isopach maps of volcanic and sedimentary units of Yucca Flat presented later. Portions of this system have been referred to as the Gravity High and Topgallant faults; however, because of the likelihood that these faults form a continuous system of which the Carpetbag fault is probably part, it will here be referred to as the Carpetbag system. The Carpetbag fault system may continue north via the northeast-trending Boundary fault found at the extreme northern terminus of Yucca Flat (Plate I), which coalesces with the Yucca/Butte fault system (Orkild et al., 1983)

or may become part of the Tippinip system, which continues on strike with the Carpetbag system into the range north of Yucca Flat (Plate I). It is likely that the Yucca and Carpetbag faults represent renewed movement along planes of weakness associated with major thrust faults underlying the basin which have been propagated upward through the Cenozoic section. On Yucca Mountain located approximately 25 km southwest of Yucca Flat, faults with northerly trends have exhibited evidence for movement prior to 12.5 myBP (R. Scott, pers. comm., 1983). Due to the complexity of interpretation of the area in close proximity to the erupting and subsiding caldera complex, it is difficult to determine what implication this group of faults may have for the regional stress field at this time. However, if pre-existing flaws have been reactivated beneath Yucca Mountain, as has been suggested for Yucca Flat, the displacement on these faults may be accounted for by a variety of stress orientations.

NORTHEAST FAULTS

In contrast to the north-south faults that are buried in Yucca Flat, the northeast-trending Mine Mountain and Cane Spring faults traverse the ranges and offsets can be directly observed. Several Tertiary volcanic units, the Ammonia Tanks and Rainier Mesa Members of the Timber Mountain Tuff and members of the Paintbrush Tuff exhibit left-lateral offset across the Mine Mountain fault just east of Mid-Valley (Plate I), where the contacts between units intersect the fault at right angles. Approximately 1.4 km of left-lateral slip and 0.25 km of dip-slip motion occurs at this point (Orkild, 1968).

Left-lateral movement occurred sometime after deposition of the Ammonia Tanks Member, or after ~11 myBP.

The Cane Spring fault system also shows very little dip-slip displacement (~0.2 km) and practically no thickening of units on the down-dropped side (Poole et al., 1965). Possible left-lateral offset of basalt contacts across the Cane Spring fault indicate 1.3 km of left-lateral offset (Poole et al., 1965; Ekren and Sargent, 1965). This evidence for left-lateral slip is hardly as compelling as that on the Mine Mountain fault due to erosional considerations, but it is interesting to note the similarities in implied offset; a ratio of 1:6.5 dip-slip to strike-slip on the Cane Spring fault and a ratio of 1:5.6 on the Mine Mountain fault. The age of the basalt is unknown but probably ranges from 8-10 myBP (D. Vaniman, pers. comm., 1983).

The Rock Valley fault also exhibits evidence for left-lateral offset where outcrops of the Pavits Spring Formation in central Rock Valley appear to be displaced with respect to each other across the inferred traces of the Rock Valley fault. It is difficult to estimate any vertical displacement on this segment of the fault due to the lack of horizontal markers observed in the outcrops. However, if pure strike-slip motion is inferred, as much as 1.9 km of left-lateral offset may have occurred.

The intervening faults between these northeast faults appear to form an "S" pattern (Figure 7, Plate I). This configuration, which is particularly noticeable between the Cane Spring and Mine Mountain faults, suggests the presence of Riedel and conjugate Riedel shears

(Tchalenko and Ambraseys, 1970) formed at the initiation of a zone of left-lateral shear.

NORTHWEST FAULTS

Some northwest faults have been reported on Yucca Mountain but these faults were primarily active before 11.1 myBP because the distribution of the Rainier Mesa Member is not effected by them (R. Scott, pers. comm., 1983). Local northwest-trending as well as north-trending basalt dikes dated approximately 10 myBP have been mapped in this area indicating that fault planes of these orientations were probably in existence by this time. Major northwest faults are not observed in the Yucca Flat area and no northwest-trending recent cracks have been observed in the alluvium, further indicating that they have not played a major role in the tectonic history of NTS after ~11 myBP. In general, northwest-trending faults found in the ranges seem to have been disrupted by north-south and northeast faults which apparently were initiated or increased in activity after movement on northwest-trending faults had waned.

CORRELATION OF FAULTS WITH STRESS FIELDS

Carr (1974) postulated a present-day extension direction of N50°W for the NTS. This was derived from northeast-trending explosion related fractures, northeast-trending tectonic cracks in Yucca Lake playa sediments, earthquake first-motion studies, in situ strain measurements, and northwest-southeast drill hole enlargements in Yucca Flat. Current work at Yucca Mountain in conjunction with the Nevada

Nuclear Waste Storage Investigations (NNWSI) has involved more in situ stress measurements. The least principal stress direction calculated from this study is N60°W (J. Stock, pers. comm., 1983).

The difference may be explained by the following relations. Yucca Mountain is composed of a very thick section of volcanics on the southern extremity of the caldera complex. Measurements at depth beneath Yucca Mountain may actually reflect a residual stress field formed as a result stresses locked in during the thermal history of the rock sequence (Jaeger and Cook, 1969; Englander and Sbar, 1976). The possible consequences of such a relationship are poorly understood and whether or not a volcanic pile might be so influenced is not clear. The N50°W extension direction might then be supposed to be more representative of the present day stress field because it has been derived from a variety of observations in various locations. These observations include cracks and elongation of drillholes found in Tertiary-Quaternary alluvium; young, surficial manifestations which are probably entirely the result of modern stresses. Also,the alluvium has not been subjected to high thermal regimes which may possibly render the tuffs more susceptible to retention of stress orientations associated with the previous history of the rock, as may have occurred in the tuffs at Yucca Mountain where the N60°W measurement was observed.

Although it is obvious that the north-south faults have been present and active since pre-tuff time, it appears that the northeast faults are of more recent origin. The presence of sigmoidal fault patterns that resemble Riedel shears and intervening conjugate Riedel

shears are strongly indicative of this since the Riedel shears are intimately related to initial stages of shear zone formation (Tchalenko and Ambraseys, 1970). Wilcox et al. (1973) describe features associated with wrench faults including fractures which intersect the wrench zone at low angles (synthetic) and those at high angles (antithetic) which have been termed Riedel shears and conjugate Riedel shears, respectively (Tchalenko, 1970). In actual fault studies, the synthetic fractures occur at 10-30° to the main strike-slip fault and the antithetic fractures intersect the main fault at between 70° - 90°. In a left lateral zone, the effects of internal rotation due to wedging and external rotation due to strike-slip faulting are cancelled out on the synthetic faults, leaving them essentially parallel to the fault zone; whereas, the antithetic faults rotate in a counterclockwise sense due to the external rotation. This causes the antithetic faults to become bent into an "S" pattern (Wilcox et al., 1973), as is observed on the intervening faults between the left-lateral northeast faults at NTS. Tchalenko (1970) has described the step by step evolution of wrench zones in clay. In his model, Riedel and conjugate Riedel shears form immediately before peak shearing resistance is reached. The Riedel shears then begin to rotate into the plane which will eventually become the plane of principal strike-slip displacement. Late in the history of shearing, at the point of almost 100% extension, the fractures eventually coalesce into a thin zone or a single plane along which nearly all of the movement occurs. The northeast-trending faults south of Yucca Flat form essentially a single plane which would point to a late stage of development. In the case of clay modeling, this

would indicate 100% extension; however, differences in rheology and inhomogeneities present in the actual fault zone may not allow direct comparison. Although some of the early-formed fractures rotate into the primary fault plane, Wilcox et al. (1973) state that the conjugate Riedel shears continue to operate becoming most strongly influenced by the extensional component of the deformation. The resulting displacement is almost wholly vertical, so it is certainly reasonable that these features continue to be observable on the surface at NTS. In addition, portions of these original conjugates are oriented such that the modern stress direction of N50W is favorable for their continued vertical displacement. Such features are commonly observed between related strike-slip faults (Wilcox et al., 1973).

The orientation of least principal stress for the northeast-trending faults, derived using the Coulomb shear failure criteria, would be approximately N80°W-N85°W (Jaeger and Cook, 1969). A modern extension direction of N50°W is almost perpendicular to these faults so their resultant movement should be almost entirely dip-slip; lateral movement should be minimal or nonexistant. The present stress field is obviously incompatible with the large left-lateral component of displacement present or with the initial stages of development of these faults. The stress field must have rotated to the present N50°W orientation sometime after much of the movement on the Cane Spring and Mine Mountain faults had occurred between about 11 myBP and the present.

THREE-DIMENSIONAL ANALYSIS OF YUCCA FLAT

Data from over 300 drill holes in Yucca Flat were used to construct isopach and structure contour maps of major Tertiary and Quaternary units. The units shown were chosen primarily for ease of identification. Facies relationships have been imperfectly understood in the past and on-going work (R. Warren, pers. comm., 1983) is just now beginning to unravel many complex relationships between rocks described in various locations at NTS. The maps were consequently constructed using time contemporaneous groupings rather than individual formations or members. The maps referred to in the text below are generalized from Plates II-X. The plates show all of the data points used to construct the isopachs and structure contours. The heavy lines on these maps represent the surface manifestations of major faults observed in Yucca Flat.

Figure 8 shows an isopach of all volcanic units underlying Yucca Flat beneath the Grouse Canyon Member (Table 2). These rocks range in age from approximately 30 to 13.8 myBP. The units included are Tunnel Bed 4, Tunnel Bed 3, the Tub Spring Member, the Tuff of Yucca Flat, Tunnel Bed 2, Tunnel Bed 1, the Fraction Tuff, the Red Rock Valley Tuff, and other unidentified tuff units (Table 2). Although this represents a very long time span, these units have been lumped together both because of the paucity of data from the lower units and also because of recent work that indicates previously accepted identification and correlation of sections of this lower sequence is incorrect (R. Warren, written comm., 1984). The isopach shows the presence of a
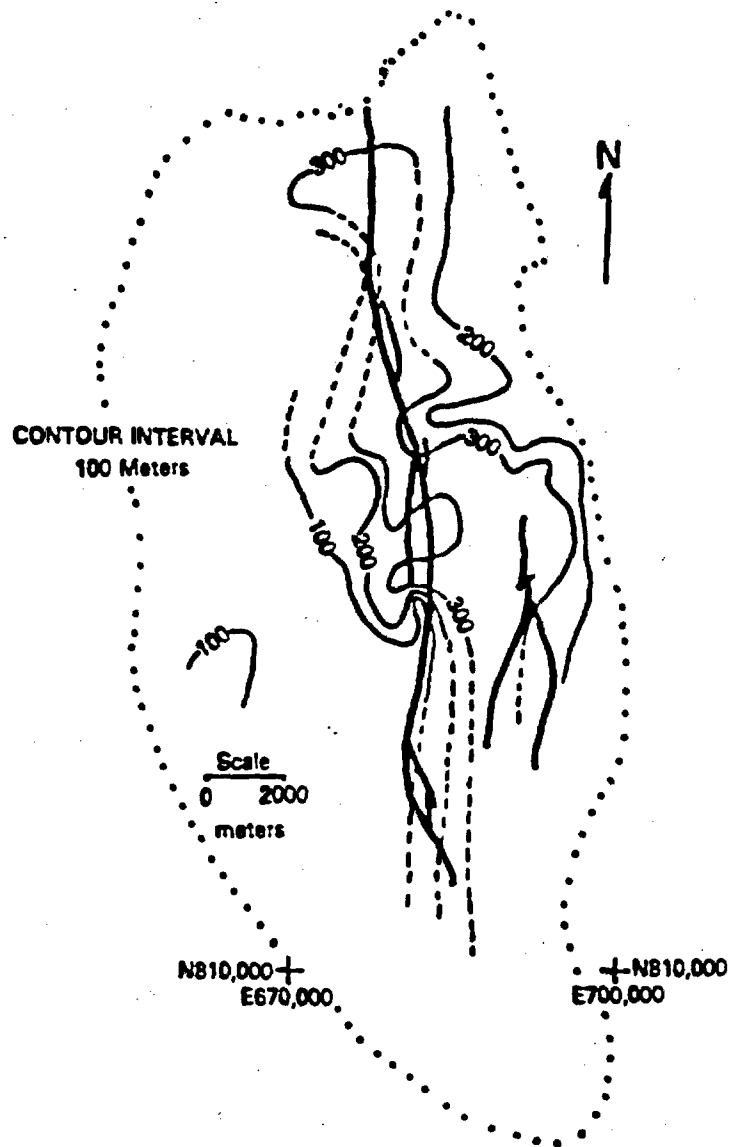
Figure 8. Isopach map of tuffs older than the Grouse Canyon Member. Stipple indicates outline of Yucca Flat basin; heavy lines are fault surface traces.

north-northwest-trending valley or depression. However, the present surface trace of the Yucca Fault does not interrupt the isopachs and, therefore, did not influence the deposition of these tuff units. This argues for inactivity along the fault at this time.

The isopach of the Grouse Canyon Tuff (13.8 myBP) was constructed because, even though it is a relatively thin unit, the distinctive peralkaline tuff is an easily recognizable marker (Figure 9). Although the isopachs are discontinuous, there is a maximum of 40 meters displacement possible. Ten meters may be a more reasonable figure when the possibility of right-lateral shift of the isopachs along the Yucca fault is taken in account. It must be pointed out that, although the data are truncated at the present trace of the Yucca fault on this particular construction, a variety of fault orientations not related to the Yucca Fault can fit the data. Also, the Carpetbag system which is thought to be temporally related to the Yucca system shows no evidence of activity. Thus it is unlikely that the Yucca fault was active before or during deposition of the Grouse Canyon tuff.

The Paintbrush Tuff sequence as shown on Figure 10, includes several volcanic units emanating from various locations within the time period 12.5-13.5 myBP. The sequence includes the Paintbrush Tuff, the Area 20 Tuff, the Wahmonie-Salyer Volcanics, and the Crater Flat Tuff. The isopachs are much more irregular, suggesting the possibility of a complex faulting situation. Faults found truncating the Paintbrush sequence appear to have a variety of orientations and many are traceable via drillhole data into the alluvial section where they have comparable displacements and, therefore, became active long after
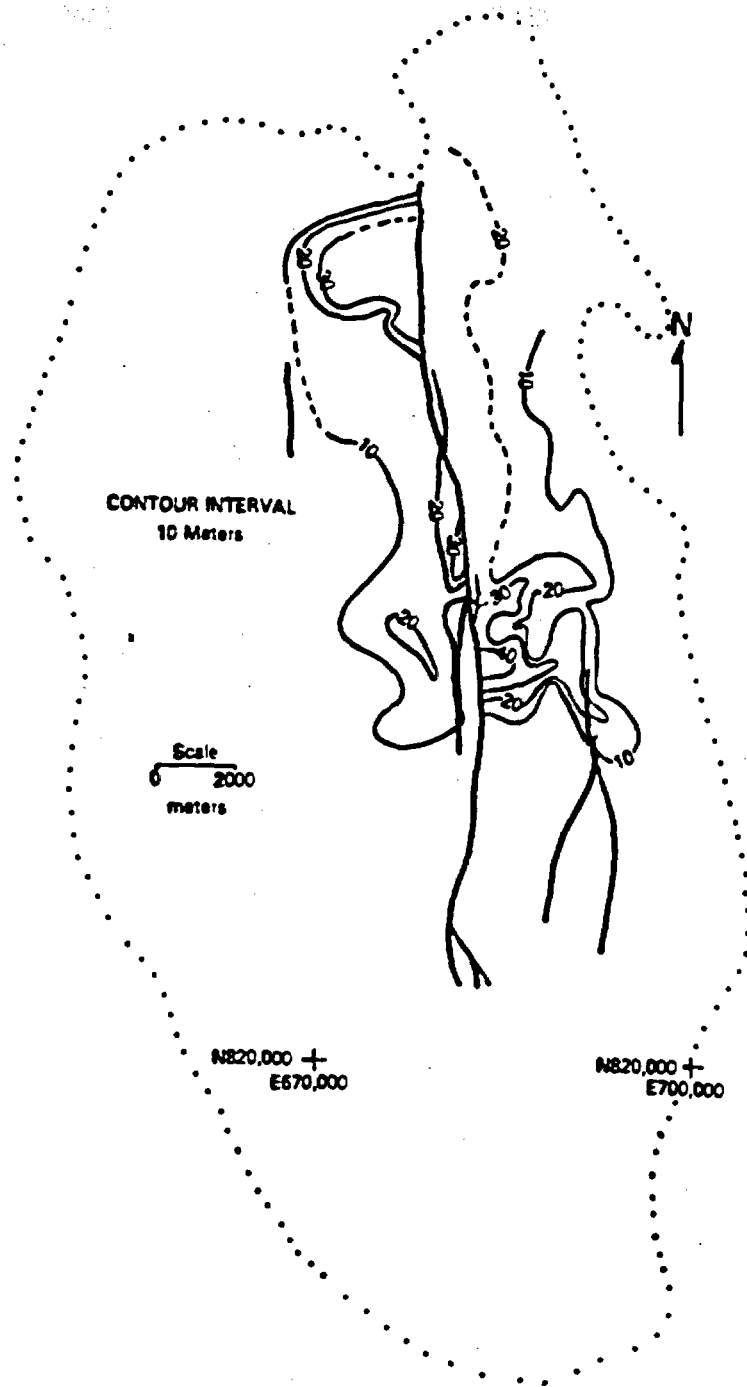
Figure 9. Isopach map of the Grouse Canyon Member, Belted Range Tuff. Stipple indicates outline of Yucca Flat basin; heavy lines are fault surface traces.
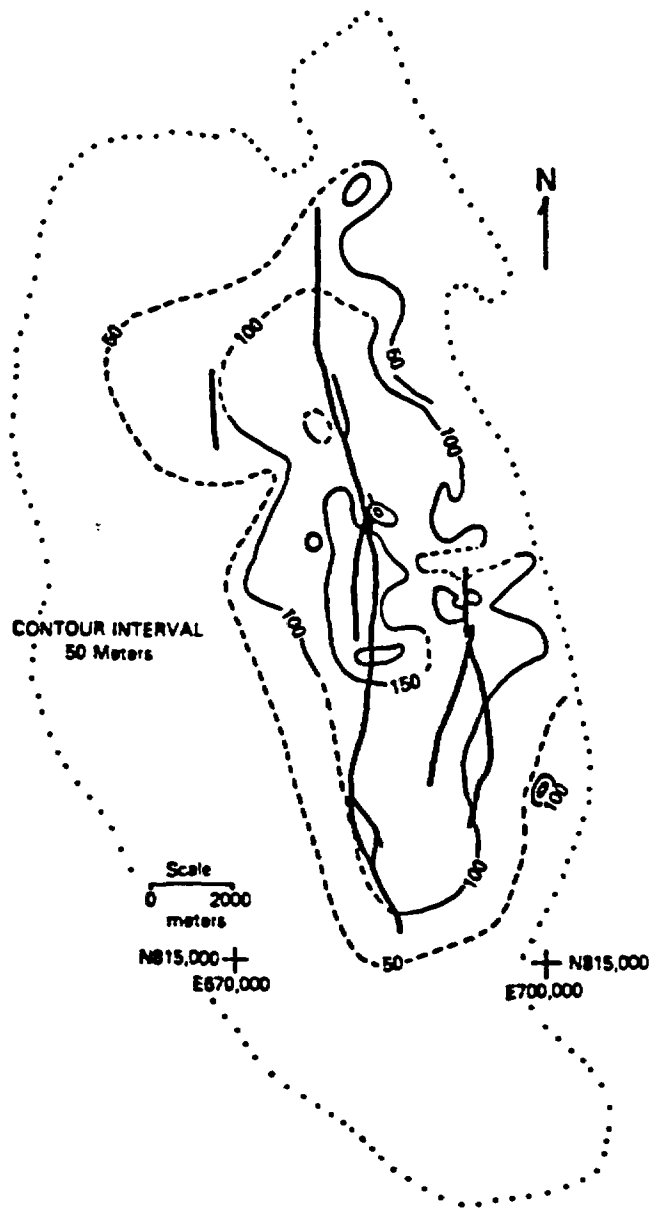
Figure 10. Isopach map of the Paintbrush Tuff. Stipple indicates outline of Yucca Flat basin; heavy lines are fault surface traces.

Paintbrush deposition. Tectonic activity is reported on northwesterly and north-south faults at Yucca Mountain, 40 km southwest of Yucca Flat (Robert Scott, written comm., 1984) during this time. In Yucca Flat, however, the north-south-trending Yucca and Carpetbag faults again fail to indicate offset.

The last volcanic unit shown is the 11.1 myBP Rainier Mesa Member (Figure 11). No displacement during Rainier Mesa time is observed on either the Carpetbag or Yucca faults as indicated by the continuous isopach distributions.

The isopach of Tertiary and Quaternary alluvium (Figure 12) shows a dramatic change in the character of the basin. The north-south faults have become active and the thickened alluvium indicated by the isopachs has accumulated on the down-dropped side of these faults. An very thick sequence of alluvium (1161 meters) is observed at the southern end of Yucca Flat between the Yucca and Carpetbag faults.

The structure contour maps shown in Figures 13-16 were drawn on the base of each unit. Offset along the Yucca fault does not increase down-section which supports the proposition that it was not continuously active during the deposition of all of the Cenozoic units. No evidence is found here for the presence of major faults other than the Yucca or Carpetbag. Also, there are no cross-cutting trends that might indicate control of rock distribution by major faults other than the Yucca and Carpetbag at any time during the deposition of these units.
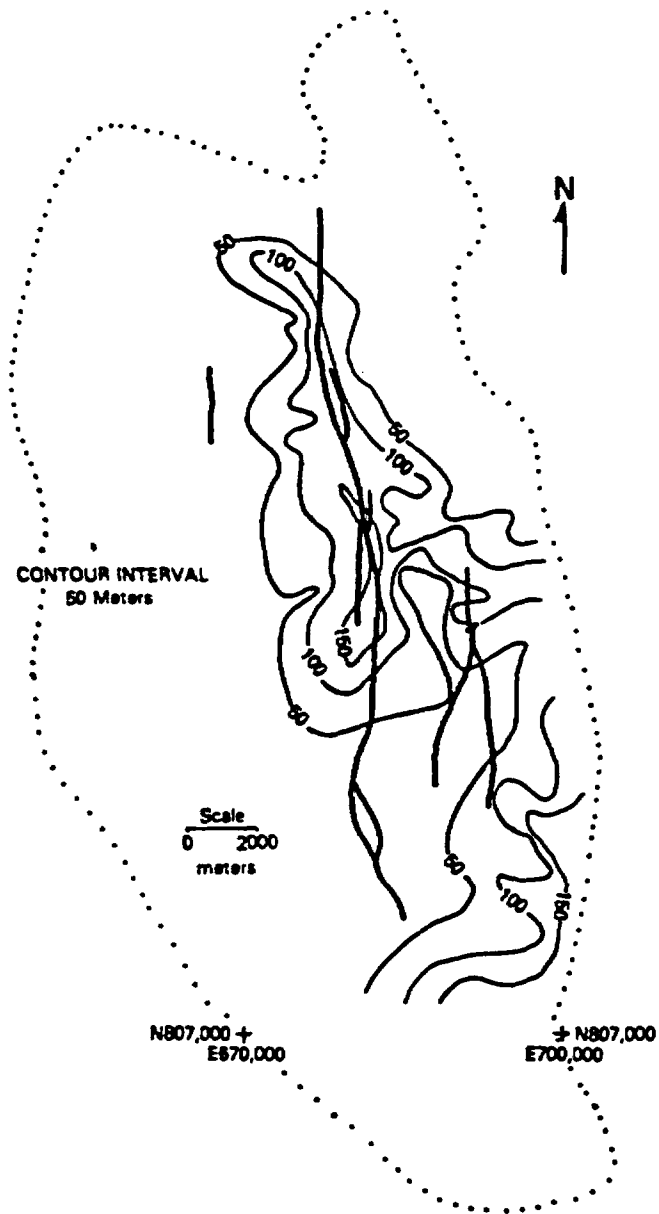
Figure 11. Isopach map of the Rainier Mesa Member, Timber Mountain Tuff. Stipple indicates outline of Yucca Flat basin; heavy lines are fault surface traces.
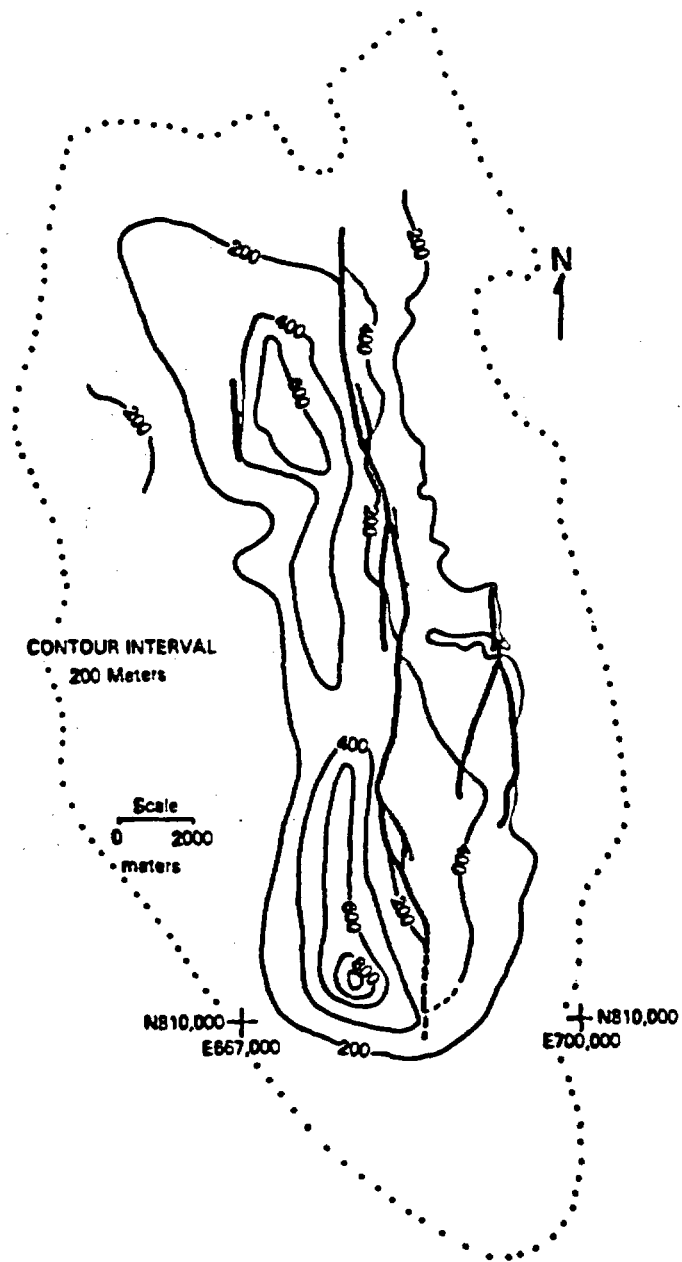
Figure 12. Isopach map of Tertiary-Quaternary alluvium. Stipple indicates outline of Yucca Flat basin; heavy lines are fault surface traces.
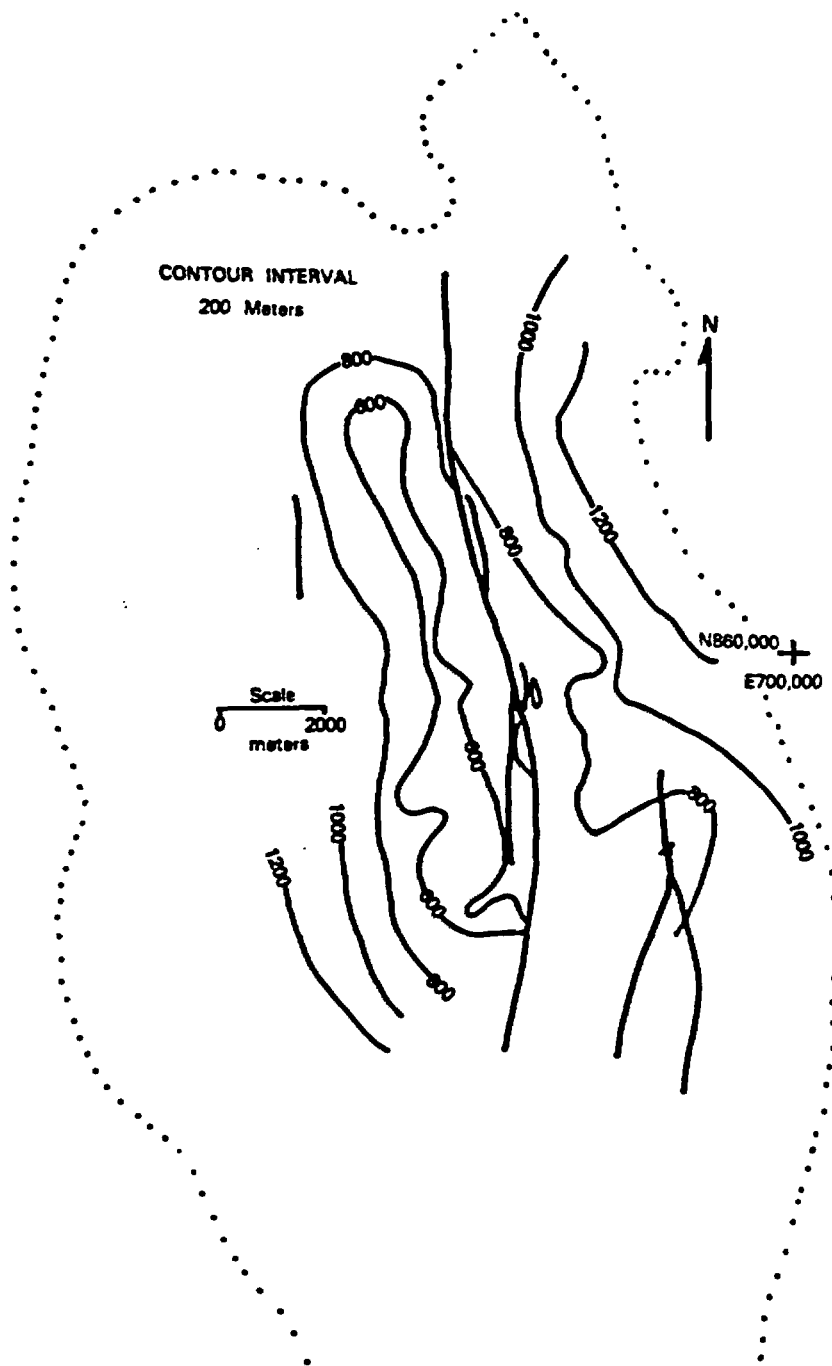
Figure 13. Structure contour map on the base of the Grouse Canyon Member, Belted Range Tuff. Stipple indicates outline of Yucca Flat basin; heavy lines are fault surface traces.
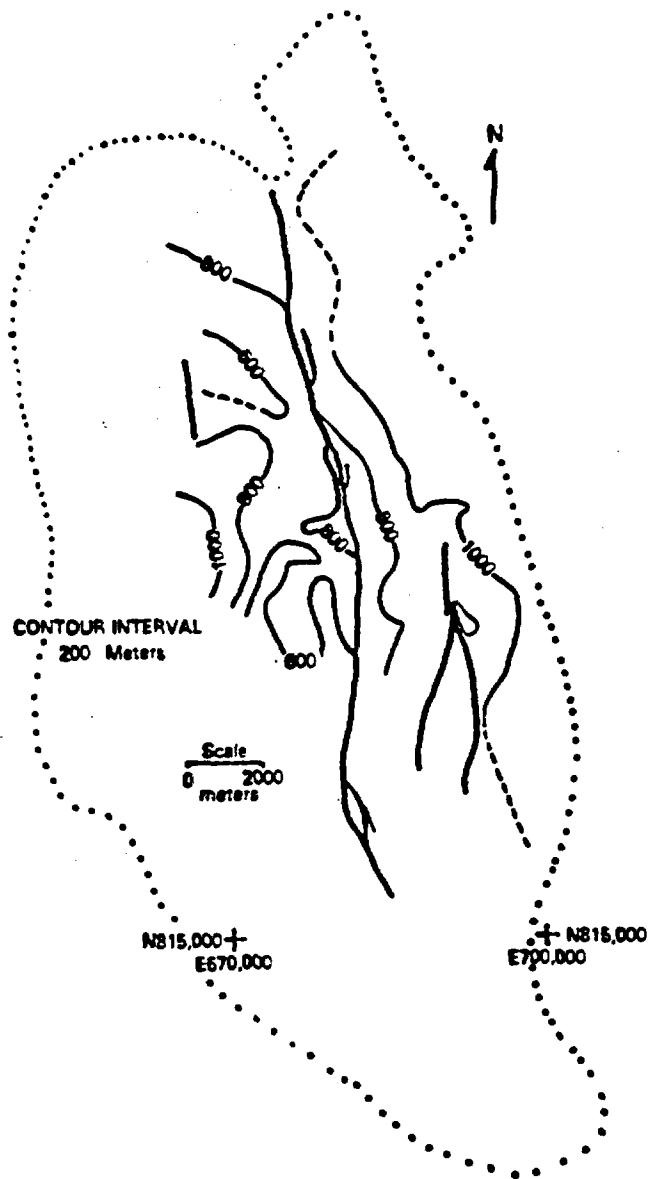
Figure 14. Structure contour map on the base of the Paintbrush Tuff. Stipple indicates outline of Yucca Flat basin; heavy lines are fault surface traces.
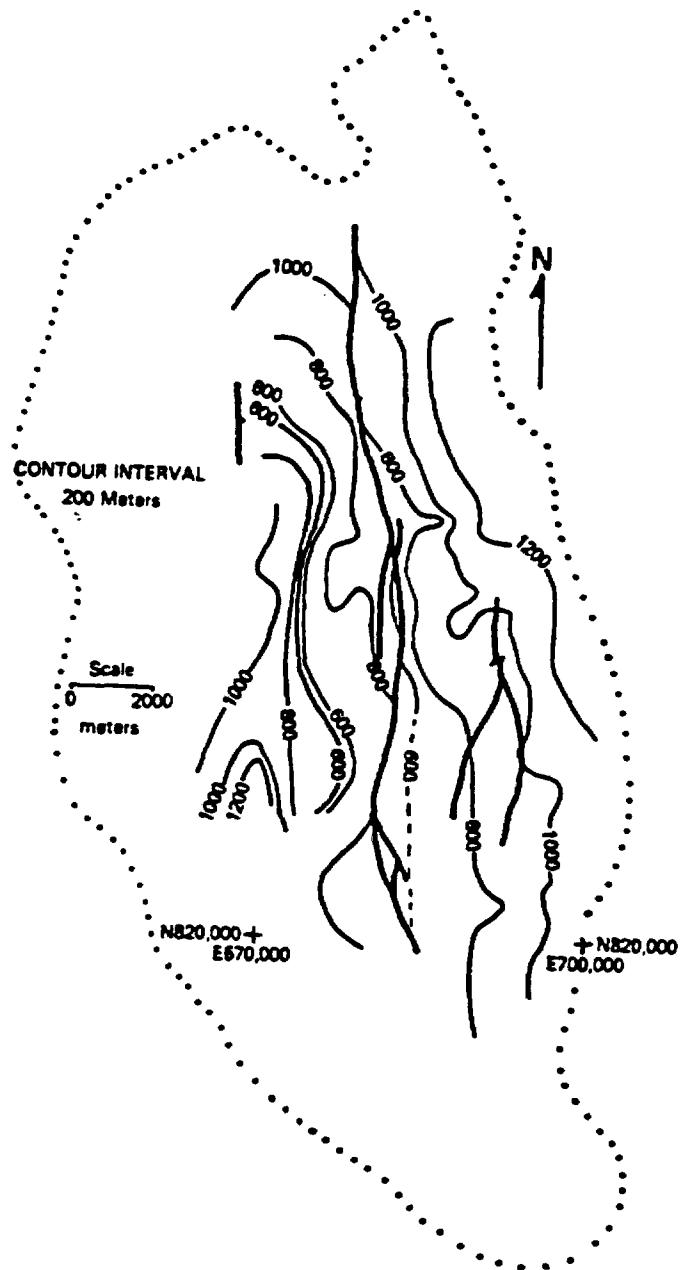
Figure 15. Structure contour map on the base of the Rainier Mesa Member, Timber Mountain Tuff. Stipple indicates outline of Yucca Flat basin; heavy lines are fault surface traces.
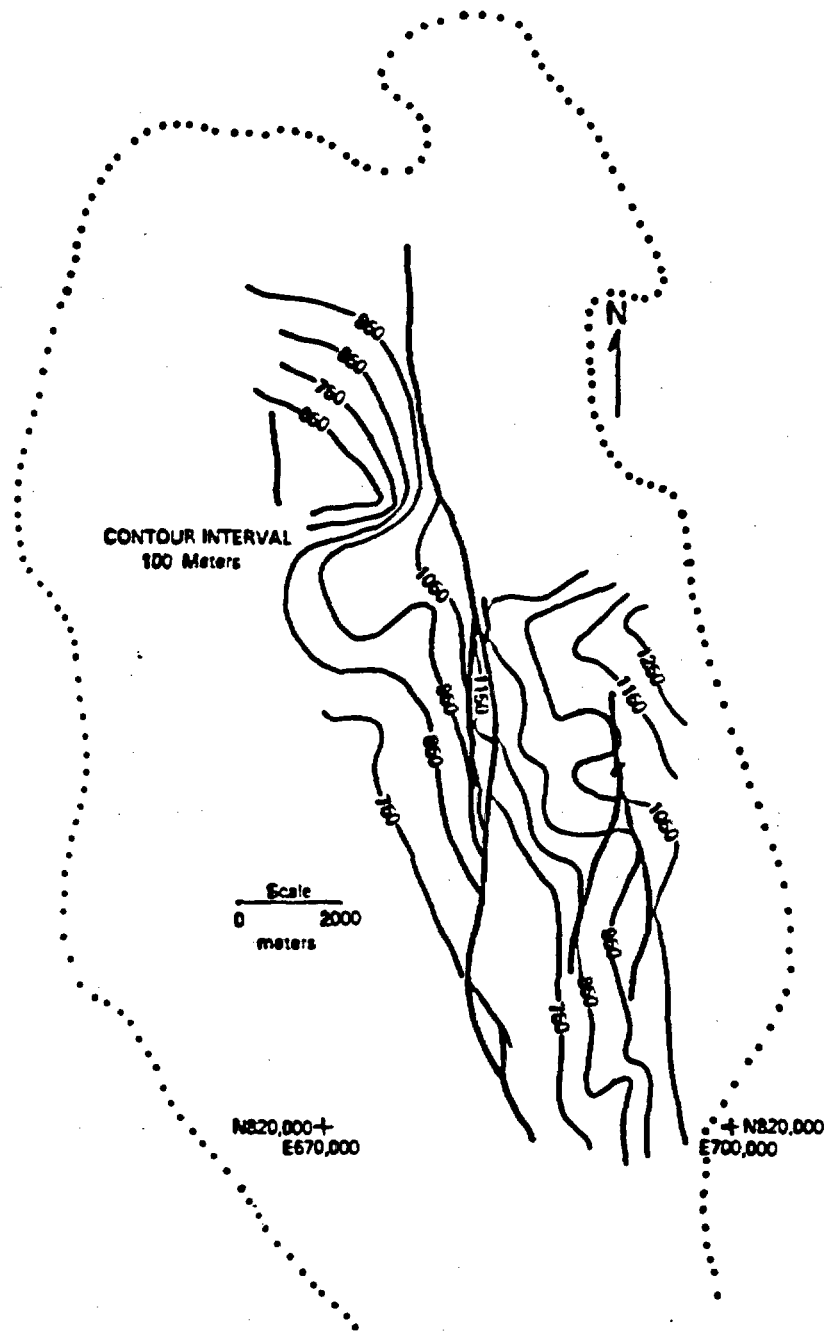
Figure 16. Structure contour map on the base of the Ammonia Tanks Member, Timber Mountain Tuff. Stipple indicates outline of Yucca Flat basin; heavy lines are fault surface traces.

SLICKENSIDE ANALYSIS

Approximately 200 slip lineations were measured on major fault zones at NTS. The primary faults from which data were collected include Cane Spring, Mine Mountain, Jangle Ridge-Paiute Ridge, and Boundary. Other sites were chosen because of their proximity to major fault zones. The number of measurements varies greatly from location to location because many of the rock types found at NTS are not conducive to formation or retention of slickensides on fault surfaces. The partially welded ash flow tuffs and bedded tuff sequences were particularly poor in this regard. However, volcanic breccias and densely welded ash flows yielded much good data. A complete listing of slip data occurs in Appendix I.

In general, fault trends are very poor indicators of the stresses operating through time. There tends to be a fairly consistent angular relationship between the stress orientation and the resultant fault set at the time of formation (Jaegar and Cook, 1969). But after the point of failure, the plane of weakness can continue to move in a wide variety of stress orientations. Slickensides, however, record movement in a single stress environment. On normal faults they roughly indicate the intersection of the fault plane and the least principle stress plane. For this reason, slip lineations are much better approximators of changes in stress fields than are fault trends.

Areas of brittle deformation have major faults acting as localized areas of deformation. It is much easier to determine the stress tensor acting in such a regime as opposed to regions of plastic

deformation where pressure, temperature, and external rotations cause a complex relationship between stress and the resulting deformation (Etchecopar et al., 1981). Angelier (1979) has developed a computer technique for analyzing slickenside data in such a brittle regime. The program determines the least squares fit deviatoric stress tensor from slip lineations measured in the field. A mean stress tensor is computed minimizing the components of calculated tangential (shear) stresses perpendicular to the measured striations. A minimum of four independent fault sets is required to perform the inversion (M. L. Zoback, written comm., 1983). An option for weighting data on the basis of relative value of data points determined by field observation exists in the computer program. However the data in the study were not analyzed using the weighting option because there was no obvious difference in the quality of data collected.

The data input requires three fault slip geometry measurements. It is in the following format that slip data in Appendix I are presented. The first, dip direction, is represented by an azimuthal angle of 0° to 360° (90° from the strike direction). This method eliminates ambiguity introduced by using strike. Second is fault dip measured between 0° to 90° from horizontal. Finally, slip angle or pitch, which is the angle between the lineation and the horizontal measured in the plane of the fault. The slip angle ranges from -180° to +180° and relative motion is determined by the following rules: negative angles of 0° to -180° are components of normal slip; positive angles of 0° to +180° are components of reverse slip; left-lateral components range between 0° to 90° and 0° and -90° where 0° is pure

left-lateral slip; right lateral components range between 90° and 180° and -90° and -180° where +180° or -180° is pure right-lateral slip; 90° is pure dip-slip. The first characters (up to 7) indicate station numbers, in this instance keyed to U.S.G.S. 7-1/2 minute geologic quadrangle maps.

During the course of data analysis, data points with high discordance to the derived stress tensor were removed. Figure 17 shows the last steps of the iterative process from the direct analytic modeling: (A) shows the point at which all but 3.64% of the points fit the model shown in which S_1 = greatest principle stress, S_2 = intermediate principle stress, and S_3 = least principle stress. (B) and (C) demonstrate the rotation of the stress orientations as greater accord is reached with the data. Finally (D) shows the model which was accepted. Although the sense of slip does not reach 100% agreement, i.e. 0% with the wrong sense of slip, it became very difficult to discern which data points should be removed. In any event, the adjustment of one or two points should not make a great deal of difference in the final calculation of the stress state. This process was repeated until essentially 100% agreement between all data points and the stress tensor derived by inversion was achieved. Using the method the following results were obtained: 131 data points (approximately 68% of all data analyzed) fit a N78°W extension; 38 points (approximately 20%) fit a S87°W extension; and 25 points (approximately 13%) could not be determined to fit any single extension direction (Figure 18). Visual inspection of the three data sets as divided on the basis shown above show no obvious correlation between

3.64% WRONG SENSE OF SLIP

$S_1=103,87$

$S_2=358,1$

$S_3=268,3$

(A)

3.11% WRONG SENSE OF SLIP

$S_1=122,86$

$S_2=5,2$

$S_3=275,4$

(B)

2.61% WRONG SENSE OF SLIP

$S_1=127,86$

$S_2=10,2$

$S_3=280,3$

(C)

1.54% WRONG SENSE OF SLIP

$S_1=119,88$

$S_2=12,1$

$S_3=282,2$

(D)
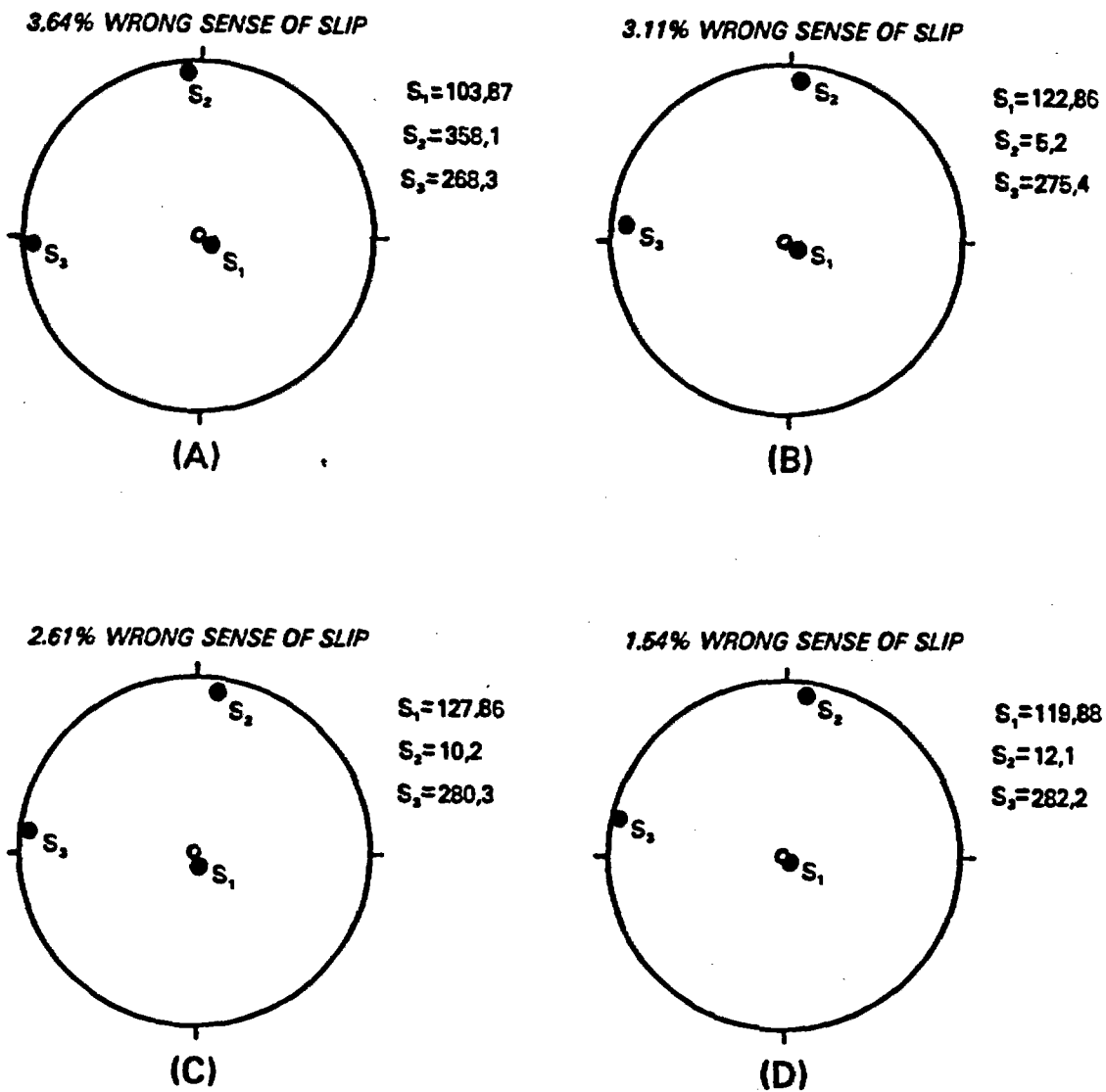
Figure 17. Successive results of direct analytical analysis. For explanation see text.
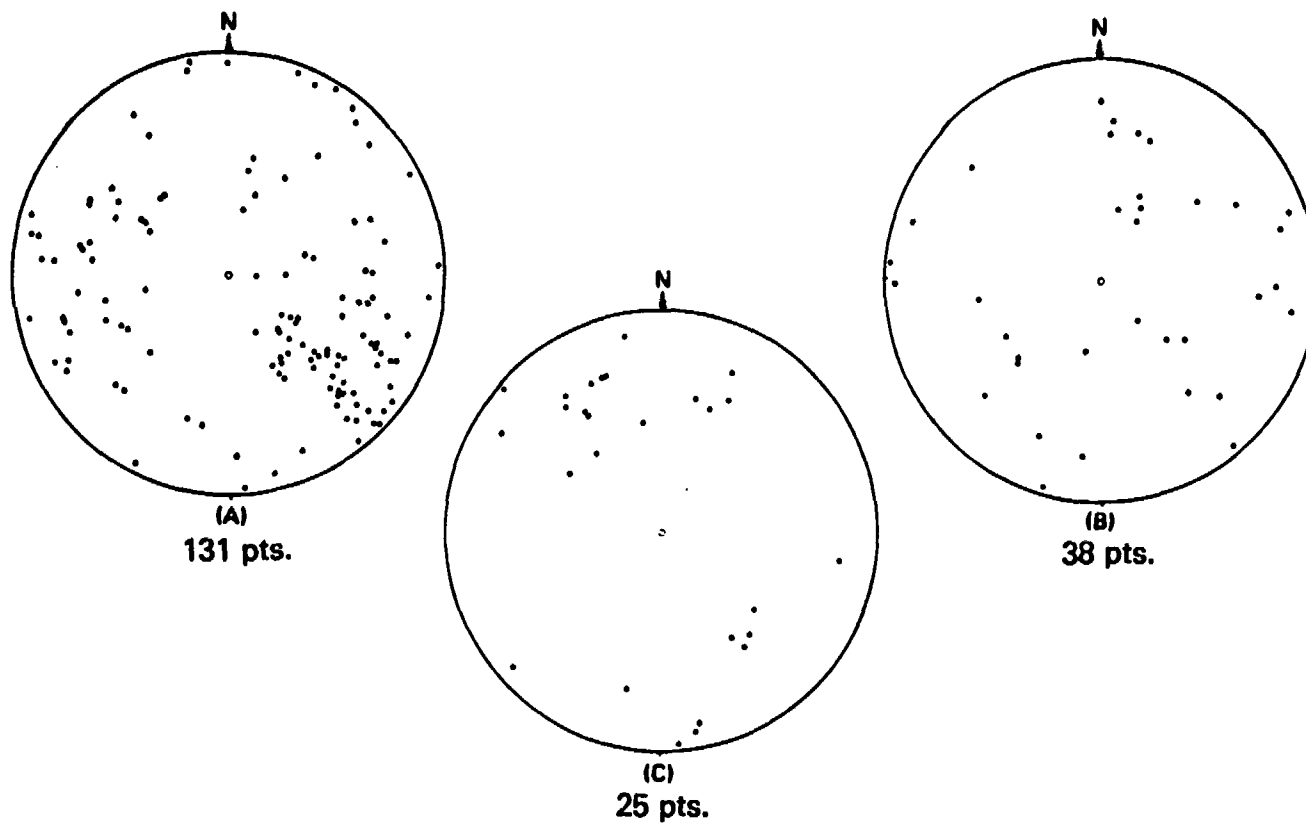
Figure 18. Lower hemisphere, equal area net showing poles to fault planes of faults responding to a given extensional stress direction, number of data points used to derive the individual stress tensors also shown: (A) = N78°W, (B) = S87°W, (C) no fit.

any one fault zone or orientation with one extension direction; faults with a wide variety of trends had striae consistent with the N78°W and S87°W extensions. The northeast-trending girdle in the last set of data may simply be the result of the small number of data points.

DISCUSSION AND CONCLUSIONS

Rotation of the least principal stress clockwise from ~N78W to ~N50°W in the Yucca Flat area of NTS is demonstrated by fault patterns and displacements. Slickenside data also show that faults at NTS have moved in response to a more westerly-directed extension direction than that observed today. Left-lateral displacement on the Cane Spring and Mine Mountain faults, which occurred after 11 myBP, provides an indication of the age of the older stress field. The deep section of alluvium in southern Yucca Flat can also be used to determine age of movement on the fault systems in response to the different stress orientations.

The occurrence of the deep alluvial trough at the inner curve of the bend where the northeast faults become continuous with the northerly-trending faults allows the following scenario. In the older west-northwest extensional stress field, the northeast faults would be strongly left-lateral and the north-south faults would be primarily dip-slip in nature with some right lateral component (Figure 19). Right-lateral movement has been proposed for north-northwest trending faults between the CP Hogback (Figure 2) and the adjacent range (Plate I) (Carr, 1974). At the inner curve where opposing senses of strike-slip displacement operate, an extremely deep depression or pull-apart might be expected just as occurs in Yucca Flat (Figure 19). The N78°W extension then would have been operative from sometime after 11 myBP and concurrent with much of the alluvium deposition in Yucca Flat. The subsequent rotation to N50°W must have occurred very

YUCCA FAULT

PULL-APART
BASIN
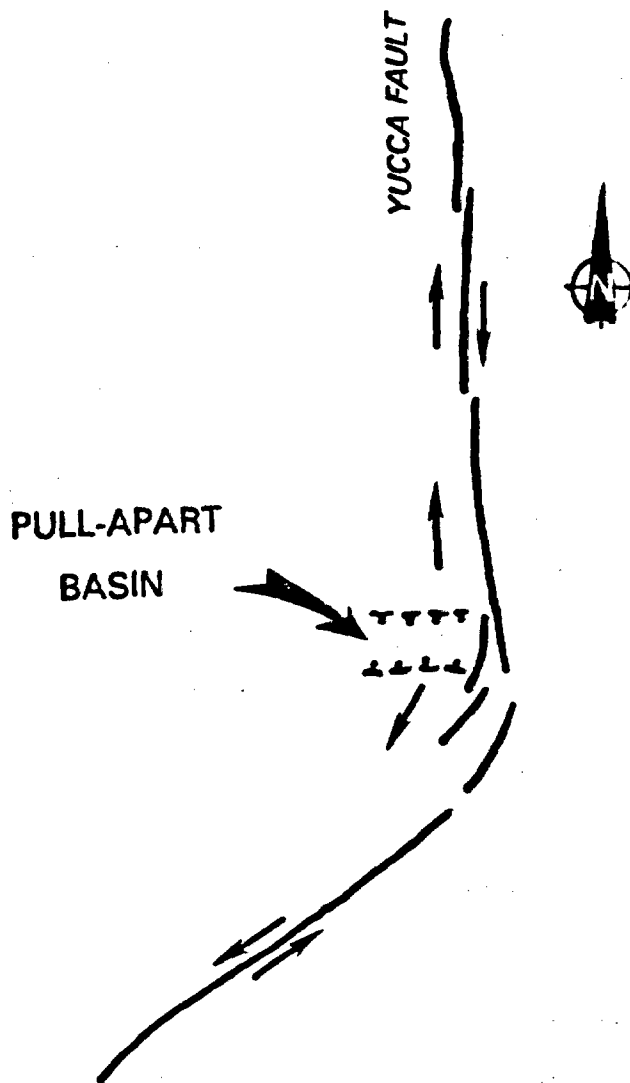
Figure 19. Interaction of north-south fault with right-lateral
movement and northeasterly fault with left-lateral movement
forming deep alluvial trough.

recently. This is supported by the fact that very little dip-slip displacement is found on the northeast faults. These faults have experienced little or no dip-slip offset by the present stress despite the fact that their orientation is highly favorable for such movement.

Many studies have been conducted in the Basin and Range to determine stress directions during the Cenozoic. In most cases, models for stress field changes are derived from the premise that any given extension direction only activated fault planes normal to that direction. Wright (1977) has shown some of the problems that may arise from using this method. However, where numerous studies report activation and movement of very similarly oriented faults over a fairly large area during a certain time periods this method gains more credence. In individual studies, slickenside analyses become important in resolving unique solutions for stress directions controlling fault movement. Although local stresses and inhomogeneities may play a much larger role in determining timing and amount of displacement on some faults, a variety of such studies, indicating the presence of similar fault trends during a given time, strongly argues that they are the result of a single regional stress field. It also might be noted that individual study areas, where the amount of fault movement is reported to increase or decrease, may only indicate that displacement has moved from one group of faults to another rather than indicating a regional change in rapidity of rate extension as suggested by Speed and Cogbill, 1979 and others. This may have occurred at NTS when north-south-trending faults were active at Yucca Mountain and Pahute Mesa 12.5-13.5 myBP while faults of this orientation were dormant in Yucca Flat at

that time. Later, the north-south faults in Yucca Flat began to move resulting in very large displacements while displacements on the north-south faults to the west decreased dramatically.

West-southwest extension in the mid-Miocene has been reported in many different geographical locations in the Great Basin including: the northern Nevada rift (Zoback and Thompson,1978), west-central Utah (Anderson and Ekren, 1977) and west-central Nevada (Oldow et al., 1980; Dockery, 1982). Although extensive deformation in this stress regime has also been reported south of Lake Mead in the Eldorado and Black Mountains (Anderson, 1982) as well as along the Lake Mead fault zone and the Las Vegas shear zone; the current understanding of fault movement does not point to major fault activity near Yucca Flat during this time. However, the faults observed at Yucca Mountain and Pahute Mesa were active during this time period. Whether they are more stongly related to a regional extension field or the local stress field surrounding the caldera complex is uncertain. A portion of the slip data also gives some indication that there was fault movement near Yucca Flat in a nearly east-west extension field. Even though there is no direct evidence for the timing, this direction might be correlative with Anderson's (1982) east-west extension in southern Nevada observed about 11-5 myBP. Thus, although there is data which indicates that there may have been some movement of faults in the Yucca Flat vicinity during west-southwest or east-west directed extension around 15 to 8 myBP, the movement seems to be minor compared to that occurring later in the more northwesterly directed extension. It is interesting to note that proposed movement on the Las Vegas shear zone and the Lake Mead

fault zone as well as the majority of pyroclastic volcanic activity had ceased before the initiation of movement on faults near Yucca Flat in the new N78°W stress field. Sometime after the Miocene, the presence of west-northwest (N82°W to N65°W) extension is widely reported: post 17-6 myBP in the southern Gabbs Valley Range (Oldow et al., 1980; Dockery, 1981); post 15-6 myBP in northern Nevada (Zoback and Thompson, 1978); post 12 myBP in southeastern California (Wright, 1977), and post 11-8 myBP at NTS from this paper. From Wright's (1977) work and this study, it is evident that most of the displacement on these faults has occurred fairly recently, possibly in the last 3 to 4 myBP. It may be significant that the youngest episode of basaltic volcanism began around 3.7 myBP after a 3 million year hiatus, further indicating crustal adjustments and possible stress changes occurring during this time.

The present day stress field (N50°W) discussed in this paper is derived from very recent features. Striations along a modern fault scarp in the Cortez Mountains of northern Nevada also require a N50°W extension (Muffler, 1966). Because this stress field has become so recently active and has evinced so little fault displacement, it is unlikely that it would be widely recognized if it occurs elsewhere in the Great Basin. In this case, faults which may have moved primarily in response to the previous more westerly directed extension might be interpreted as being only active in response to the currently active stress field. This would be especially true since the pervasive faults trending north-northeast to north-south would be susceptible to dip-slip motion in the N78°W extension as well as that directed N50°W.

These lines of evidence lead to the conclusion that the stress fields within the Great Basin have undergone approximately a 90° clockwise rotation in the past 17 my, from approximately southwest to N50°W. It can be speculated that the clockwise rotation may be traced even farther back in time to before 30 myBP. Burke and McKee (1979) reported a major east-west trending graben controlling ash-flow tuff deposition in central Nevada sometime before 32 myBP. At the southern extremity of NTS it is observed that the Horse Spring Formation (⌐30 myBP) also appears to have an east-west trend and its distribution may be controlled by east-west faulting. The east-west, west-northwest, and east-northeast faults of Ekren et al. (1968) thought to have been active around 26.5 myBP might be further evidence of an almost north-south extension. If these basins were controlled by normal faults at right angles to an extensional stress, a north-south least principle stress might be extrapolated. In this instance, clockwise rotation of extension would have started before ⌐30 myBP and subtended an angle of about 130° (Figure 20).

Release of compressive stress due to decrease in the convergence rate of the subducting Farralon plate, as mentioned earlier, is consistent with intra-arc and back-arc spreading (Eaton, 1982, 1984) and seems to explain the earliest orientations of extension throughout much of the Basin and Range. However, clockwise rotation in the extensional stresses as described in this study does not support a sudden shift in the stress field at a critical point of coupling at the transform boundary as proposed by Eaton (1984). Rather, a continuous clockwise rotation seems to have occurred for at least the last 17 myBP

present

N50W

3 myBP

N78W

S87W
(NTS)

SW

N-S

17 myBP

30 myBP
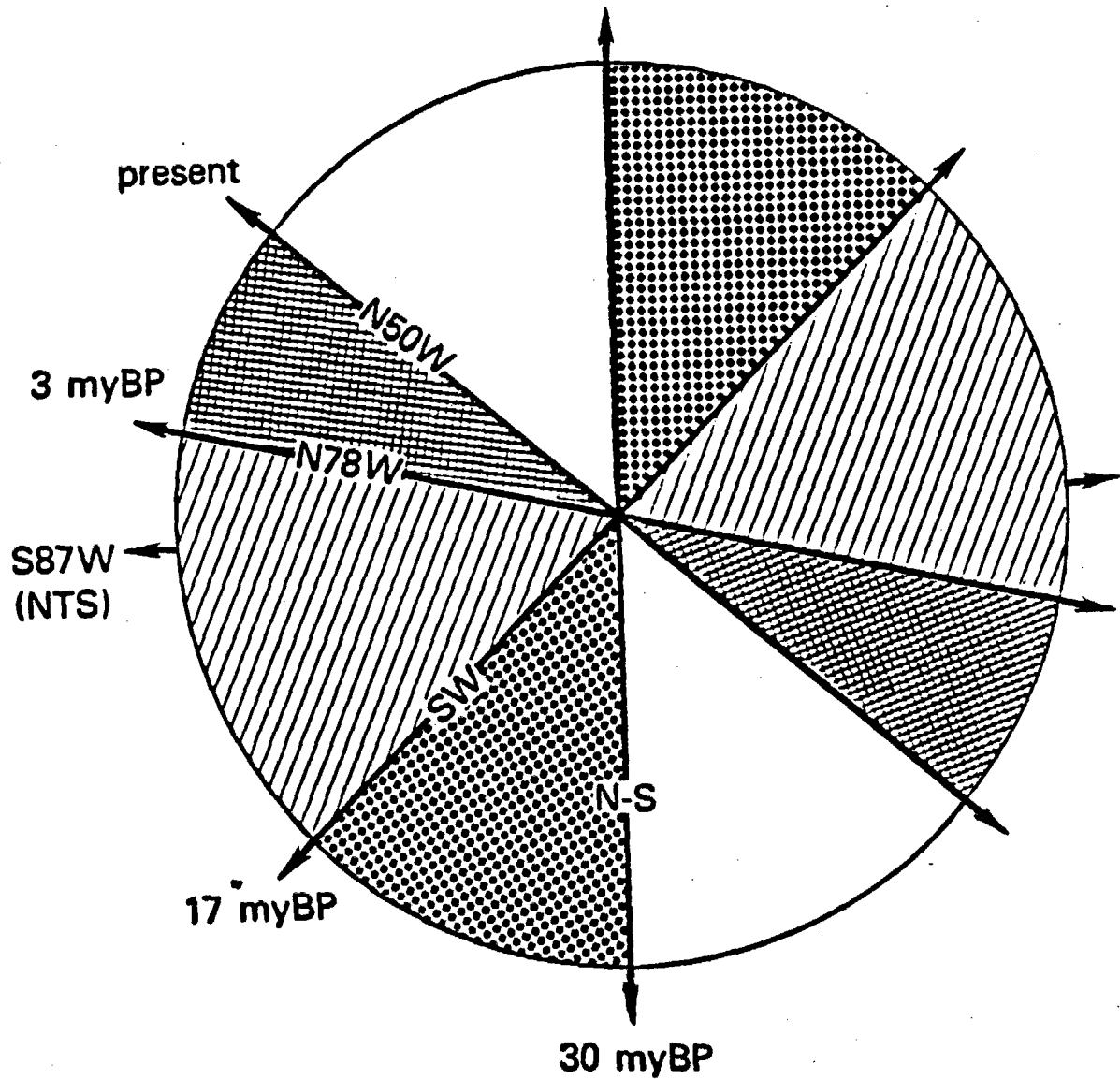
Figure 20. Postulated rotation of extensional stress directions and associated time periods generalized from regional studies. Measurement in west-southwesterly field indicates value from slickensides at NTS.

and perhaps as long as 30 myBP. In this case, it might be proposed that the transform boundary, possibly enhanced by the existence of an unstable triple junction (Ingersoll, 1982) has had a slow, but steadily increasing influence on extensional deformation essentially causing the extension direction to swing in an arc which follows the progress in the Mendocino triple junction as it travels northward. There are, of course, obvious problems with such wide sweeping scenarios depicting all areas in the Basin and Range. For instance, it would seem that at least one part of the Great Basin, the Snake Range of northeastern Nevada, has been undergoing west-northwest extension during its entire Cenozoic history of deformation (Miller, et al., 1983). Also, the southern Basin and Range Province does not seem to be affected by the rotation of least principal stress from its original west-southwest orientation. These points show that the Cenozoic development of the Basin and Range is more complex than we as yet understand it from our limited data sets.

In summary, this study has shown that normal faults in the Yucca Flat region of NTS have responded to several orientations of least principle stress during the Cenozoic. Good evidence for a N78°W extension operating post 11-8 myBP is found. This stress field then rotated very recently, perhaps within the last 3 to 4 myBP to the presently observed N50°W extension. Prior to the N78°W extension, a west-southwesterly to southwesterly extension is reported throughout much of the Great Basin and its presence is supported by slickenside data collected at NTS. In all, approximately 90° of clockwise rotation is required in the last 17 my. More tenuous evidence, in the form of

older east-west trending faults may extend this angle to 130° in the past ∿130 myBP.

REFERENCES

Albers, J. P., Belt of sigmoidal bending and right lateral faulting in the western Great Basin, *Geol. Soc. Am. Bull.*, *78*, 143-156, 1967.

Allmendinger, R. W. and Jordan, T. E., Mesozoic evolution, hinterland of the Sevier orogenic belt, *Geology*, *9*, 309-314, 1981.

Ander, H. D., F. M. Byers, P. Orkild, H. Barnes, D. Broxton, W. J. Carr, B. M. Crowe, W. Dudley, E. Jenkins, D. Krier, S. Levy, W. Hawkins, F. G. Poole, R. Shroba, R. B. Scott, D. Vaniman, M. Van de Werken, and R. G. Warren, *Nevada Test Site Field Trip Guidebook 1984, Geol. Soc. Am. Guidebook*, in press.

Anderson, R. E., Miocene structural history south of Lake Mead, Nevada-Arizona, *Geol. Soc. Am. Abst. with Prog.*, *14*, 146-147, 1982.

Anderson, R. E. and E. B. Ekren, Late Cenozoic fault patterns and stress fields in the Great Basin and westward displacement of the Sierra Nevada block: comment, *Geology*, *5*, 388-392, 1977.

Anderson, R. E., R. Fleck, and R. Bohannon, The Las Vegas Valley shear zone, Lake Mead fault system, and extensional tectonics; Lake Mead-Las Vegas region, southern Nevada, northwestern Arizona, and southwestern Utah, *Geol. Soc. Am. Abst. with Prog.*, *14*, 146, 1982.

Angelier, Jacques, Determination of the mean principal directions of stresses for a given fault population, *Tectonophysics*, *56*, T17-T26, 1979.

Armstrong, R. L., Sevier orogenic belt in Nevada and Utah, *Geol. Soc. Am. Bull.*, *79*, 429-458, 1968.

Atwater, Tanya, Implications of plate tectonics for the Cenozoic tectonic evolution of western North America, *Geol. Soc. Am. Bull.*, *81*, 3513-3536, 1970.

Bohannon, R. G., Strike-slip faults of the Lake Mead region of southern Nevada *in* Armentrout, J. M., M. R. Cole, and H. Terbest, eds., *Cenozoic paleogeography of the western United States, Pacific Coast Paleogeography Symposium 3: Pacific Section, Society of Economic Paleontologists and Mineralogists*, 129-139, 1979.

Burke, D. B. and E. H. McKee, Mid-Cenozoic volcano-tectonic troughs in central Nevada, *Geol. Soc. Am. Bull.*, *Part I*, *90*, 181-184, 1979.

Byers, F. M., W. J. Carr, R. L. Christiansen, P. W. Lipman, P. P. Orkild, and W. D. Quinlivan, Geologic map of the Timber Mountain caldera area, Nye County, Nevada, *U.S. Geol. Surv. Misc. Geol. Inv. Map I-891*, 1976a.

Byers, F. M., W. J. Carr, P. Orkild, W. D. Quinlivan, and K. A. Sargent, Volcanic suites and related cauldrons of Timber Mountain - Oasis Valley caldera complex, southern Nevada, *U.S. Geol. Surv. Prof. Paper 919*, 70 pp., 1976b.

Callian, J. T. and J. W. Geissman, Paleomagnetic data from Cretaceous plutons and their bearing on oroflexural deformation in west-central Nevada (abstract), *EOS Trans. AGU, 63*, 916, 1982.

Carr, W. J., Summary of tectonic and structural evidence for stress orientation at the Nevada Test Site, *U.S. Geol. Surv. Open File Rep., 74-176*, 53 pp., 1974.

Christiansen, R. L. and P. W. Lipman, Cenozoic volcanism and plate-tectonic evolution of western United States, II, Late Cenozoic, *Philos. Trans. R. Soc. London, 271*, 249-284, 1972.

Christiansen, R. L., P. W. Lipman, W. J. Carr, F. M. Byers, P. P. Orkild, and K. A. Sargent, Timber Mountain - Oasis Valley caldera complex of southern Nevada, *Geol. Soc. Am. Bull., 88*, 943-959, 1977.

Coney, P. J. and Reynolds, S. J., Cordilleran Benioff zones, *Nature, 270*, 403-406, 1977.

Cross, T. A., and R. H. Pilger, Jr., Constraints on absolute motion and plate interaction inferred from Cenozoic igneous activity in the western United States, *Am. J. Sci., 278*, 865-920, 1978.

Crowe, B. M. and W. J. Carr, Preliminary assessment of the risk of volcanism at a proposed nuclear waste repository within the south-central Great Basin, Nevada and California, *U.S. Geol. Surv. Open File Rep. 8-357*, 15 pp., 1980.

Davis, G. A. and B. C. Burchfiel, Garlock fault: An intra-continental transform structure, southern California, *Geol. Soc. Am. Bull., 84*, 1407-1422, 1973.

Dockery, H. A., Cenozoic stratigraphy and extensional faulting in the southern Gabbs Valley Range, west-central Nevada, M.S. thesis, Rice University, Houston, Texas, 71 p., 1982.

Drellack, S. L., W. J. Davies, J. L. Gonzales, and W. L. Hawkins, Geologic investigations of drill hole sloughing problems, Nevada Test Site, *Proceedings Second Symposium on Containment of Underground Nuclear Explosions, Kirtland AFB, Albuquerque, NM, August 2-4, 1983, Lawrence Livermore National Laboratory CONF-830882, 1*, Clifford Olsen, compiler, 271-292, 1983.

Eaton, G. P., The Basin and Range Province: origin and tectonic significance, *Ann. Rev. Earth Planet. Sci., 10*, 409-440, 1982.

Eaton, G. P., The Miocene Great Basin of western North America as an extending back arc region, *Tectonophysics*, 102, 275-295, 1984.

Elston, W. E., and T. J. Bornhorst, The Rio Grande rift in context of regional post-40 m.y. volcanic and tectonic events, *in Rio Grande Rift: Tectonics and Magmatism*, ed. R. E. Riecker, 416-38, Am. Geophys. Union, 1979.

Englender, J. T. and M. L. Sbar, Evidence for uniforn strain orientation in the Potsdam Sandstone, northern New York, from in situ measurements, *J. Geophys. Res.*, 81, 3013-3017, 1976.

Etchecopar, A., G. Vasseur, and M. Daignieres, An inverse problem in microtectonics for the determination of stress tensors from fault striation analysis, *J. Structural Geol.*, 3, 51-65, 1981.

Ekren, E. B., and K. A. Sargent, Geologic map of Skull Mountain Quadrangle, Nye County, Nevada, *U.S. Geol. Surv. Map GQ-387*, 1965.

Ekren, E. B., C. L. Rogers, R. E. Anderson, and P. P. Orkild, Age of basin and range normal faults in Nevada Test Site and Nellis Air Force Range, Nevada, *Geol. Soc. Am. Memoir 110*, 247-250, 1968.

Ekren, E. B., F. M. Byers, R. F. Hardyman, R. F. Marvin, and M. L. Silberman, Stratigraphy, preliminary petrology, and some structural features of Tertiary volcanic rocks in the Gabbs Valley and Gillis Ranges, Mineral County, Nevada, *U.S. Geol. Surv. Bull.*, 1464, 54 pp., 1980.

Fleck, R. J., Age and possible origin of the Las Vegas shear zone, Clark and Nye County, Nevada, *Geol. Soc. Am. Abs. with Prog.*, 2, 333, 1970.

Ferguson, J., Gravity analysis of Yucca Flat southern Nevada, Southern Methodist Univ., Ph.D. dissertation, p. 110, 1972.

Fernald, A. T., G. S. Corchary, W. P. Williams, and R. B. Colton, Surficial deposits of the Yucca Flat area, Nevada Test Site, *Geol. Soc. Am. Memoir 110*, 49-55, 1968.

Hardyman, R. F., Volcanic stratigraphy and structural geology of the Gillis Canyon quadrangle, northern Gillis Range, Mineral County, Nevada, Ph.D. dissertation, Univ. of Nevada, Reno, 248 pp., 1978.

Hinrichs, E. N., Geologic structure of Yucca Flats area, Nevada, *Geol. Soc. Am. Memoir 110*, 239-246, 1968.

Ingersoll, R.V., Triple-junction instability as cause for late Cenozoic extension and fragmentation of the western United States, *Geology*, v. 10, 621-624, 1982.

Jaeger, J. C. and N. G. W. Cook, *Fundamentals of Rock Mechanics*, Chapman and Hall, Ltd., New York, New York, 515 pp., 1969.

Lipman, P. W., R. L. Christiansen, and J. T. O'Connor, A compositionally zoned ash-flow sheet in southern Nevada, *U.S. Geol. Surv. Prof. Paper 524F*, 47 pp. 1966.

Lipman, P. W., H. J. Prostka, and R. L. Christiansen, Cenozoic volcanism and plate-tectonic evolution of the western United States. 1. Early and Middle Cenozoic, *Phil. Trans. R. Soc. London, A-271*, 217-248, 1972.

Longwell, C. R., Measure and date of movement on Las Vegas Valley shear zone, Clark County, Nevada, *Geol. Soc. Am. Bull., 85*, 985-990, 1974.

Miller, E. L., P. B. Gans, and J. Garing, The Snake Range decollement: an exhumed mid-Tertiary ductile-brittle transition, *Tectonics, 2*, 239-264, 1983.

Muffler, L. J., Geology of the Frenchie Creek quadrangle, north-central Nevada, *U.S. Geol. Surv. Bull. 1179*, 1964.

Naeser, C. W. and F. Maldonado, Fission-track dating of the Climax and Gold Meadows stocks, Nye County, Nevada, *U.S. Geol. Surv. Prof. paper 1199E*, 45-47, 1981.

Nelson, M. R., A Paleomagnetic investigation of oroclinal bending in the Las Vegas Range, Nevada (abstract), *EOS Trans. AGU, 64*, 686, 1983.

Noble, D. C., K. A. Sargent, H. H. Mehnert, E. B. Ekren, and F. M. Byers, Silent Canyon volcanic center, Nye County, Nevada, *Geol. Soc. Am. Memoir 110*, 65-76, 1968.

Oldow, J. S., J. N. Meinwald, and H. A. Dockery, Cenozoic high-angle fault kinematics in the Mina-Hawthorne region, west-central Nevada: uniform extension and right lateral shear, *Geol. Soc. Am. Abs. with Prog., 12*, 145-146, 1980.

Oldow, J. S. and J. W. Geissman, Oroflexural deformation in west-central Nevada reassessed: evidence from paleomagnetic data (abstract), *EOS Trans. AGU, 63*, 309, 1982.

Orkild, P. P., Geologic map of the Mine Mountain Quadrangle, Nye County, Nevada, *U.S. Geol. Surv. GQ Series Map GQ-746*, 1968.

Orkild, P. P., Geology of the Nevada Test Site, *Proceedings First Symposium on Containment of Underground Nuclear Explosions, Monterey, CA, August 26-28, Los Alamos National Laboratory Report LA-9211-C*, Hudson, B. C., E. M. Jones, C. E. Keller, and C. W. Smith, compilers, 323-338, 1982.

Orkild, P., D. R. Townsend, M. J. Baldwin, D. L. Healey, G. D. Bath, C. E. Jahren, and J. G. Rosenbaum, Geologic and geophysical investigations of Climax Stock intrusive, Nevada, *U.S. Geol. Surv. Open File Rep. 83-377*, 82 pp., 1983.

Poole, F. G., D. P. Elston, and W. J. Carr, Geologic map of the Cane Spring quadrangle, Nye County, Nevada, *U.S. Geol. Surv. Geol. Quad. Map GQ-455*, 1965.

Poole, F. G., C. A. Sandberg, and A. V. Boucot, Silurian and Devonian paleogeography of the western United States, *in* Stewart, J. H., C. H. Stevens, and A. E. Fritsche, eds., *Paleozoic Paleogeography of the western United States, Pacific Coast Paleogeography Symposium 1: Pacific Section, Society of Economic Paleontologists and Mineralogists*, 29-60, 1977.

Poole, F. G. and C. A. Sandberg, Mississippian paleogeography and tectonics of the western United States, *in* Stewart, J. H., C. H. Stevens, and A. E. Fritsche, eds., *Paleozoic Paleogeography of the western United States, Pacific Coast Paleogeography Symposium 1: Pacific Section, Society of Economic Paleontologists and Mineralogists*, 67-86, 1977.

Rich, M., Pennsylvanian paleogeographic patterns in the western United States, *in* Stewart, J. H., C. H. Stevens, and A. E. Fritsche, eds., *Paleozoic Paleogeography of the western United States, Pacific Coast Paleogeography Symposium 1: Pacific Section, Society of Economic Paleontologists and Mineralogists*, 87-112, 1977.

Ross, R. J., Ordovician paleogeography of the western United States, *in* Stewart, J. H., C. H. Stevens, and A. E. Fritsche, eds., *Paleozoic Paleogeography of the western United States, Pacific Coast Paleogeography Symposium 1: Pacific Section, Society of Economic Paleontologists and Mineralogists*, 19-38, 1977.

Sargent, K. A., and J. H. Stewart, Geologic map of the Specter Range NW Quadrangle, Nye County, Nevada, *U.S. Geol. Surv. Map GQ-884*, 1971.

Scholz, C. H., M. Barazangi, and M. L. Sbar, Late Cenozoic evolution of the Great Basin, western United States, as an ensialic interarc basin, *Geol. Soc. Am. Bull.*, *82*, 2979-2990, 1971.

Speed, R. C. and A. H. Cogbill, Candelaria and other left-oblique slip faults of the Candelaria region, Nevada, *Geol. Soc. Am. Bull.*, *Part I, 90*, 149-163, 1979.

Stewart, J. H., Possible large right-lateral displacement along fault and shear zones in the Death Valley-Las Vegas area, California and Nevada, *Geol. Soc. Am. Bull.*, *78*, 131-142, 1967.

Stewart, J. H., Initial deposits of the Cordilleran geosyncline evidence of a Precambrian (850 my) continental separation, *Geol. Soc. Am. Bull. 83*: 1345-1360, 1972.

Stewart, J. H., Spatial variation, style, and age of Cenozoic extensional tectonics in the Great Basin, *Geol. Soc. Am. Abs. with Prog., 15*, 286, 1982.

Stewart, J. H. and J. E. Carlson, Geologic map of Nevada, *U.S. Geol. Surv. Misc. Field Studies Map MF-609*, 1978.

Stewart, J. H., J. P. Aherns, and F. G. Poole, Summary of regional evidence for right-lateral displacement in the western Great Basin, *Geol. Soc. Am. Bull., 79*, 1407-1414, 1968.

Tschalenko, J. S., Similarities between shear zones of different magnitudes, *Geol. Soc. Am. Bull., 81*, 1625-1640, 1970.

Tchalenko, J. S. and N. N. Ambraseys, Structural analysis of the Dasht-e Bayaz (Iran) earthquake fractures, *Geol. Soc. Am. Bull., 81*, 41-60, 1970.

Vaniman, D., B. Crowe, and E. Gladney, Petrology and geochemistry of hawaiite lavas from Crater Flat, Nevada, *Contrib. Mineral. Petrol., 80*, 341-357, 1982.

Vaniman, D., B. Crowe, S. Baldridge, F. Caporuscio, and E. Gladney, Late Cenozoic basaltic volcanic episodes of the south-central Great Basin, Part II: Petrology and Geochemistry, in review.

Warren, R. G., Geochemical similarities between volcanic units at Yucca Mountain and Pahute Mesa: Evidence for a common magmatic origin of volcanic sequences that flank Timber Mountain Caldera, *J. Geophys. Res.*, submitted, 1983.

Wilcox, R. E., J. P. Harding, and D. R. Seeley, Basic wrench tectonics, *Am. Assoc. Pet. Geol. Bull., 57*, 74-96, 1973.

Wright, L. A., Late Cenozoic fault patterns and stress fields in the Great Basin and westward displacement of the Sierra Nevada block, *Geology, 4*, 489-494, 1976.

Wright, L. A., Late Cenozoic fault patterns and stress fields in the Great Basin and westward displacement of the Sierra Nevada block: reply, *Geology, 5*, 388-392, 1977.

Wright, L. A. and B. W. Troxel, Summary of regional evidence for right-lateral displacement in the western Great Basin: Discussion, *Geol. Soc. Am. Bull., 81*, 2167-2174, 1970.

Zoback, M. L. and G. A. Thompson, Basin and Range rifting in northern Nevada: clues from a mid-Miocene rift and its subsequent offsets, *Geology*, *6*, 111-116, 1978.

Zoback, M. L. and M. Zoback, State of stress in the conterminous United States, *J. Geophys. Res.*, *85*, 6113-6156, 1980.

Zoback, M. L., R. E. Anderson, and G. A. Thompson, Cainozoic evolution of the state of stress and style of tectonism of the Basin and Range province of the western United States, *Phil. Trans. R. Soc. Lond.*, *A300*, 407-437, 1981.

APPENDIX I

Slickenslide data from NTS (format described in text). Station designations indicate which 7-1/2 minute quadrangles in which measurements were taken: jr = Jangle Ridge, pr = Paiute Ridge, cs = Cane Spring, pv = Plutonium Valley, sm = Skull Mountain, mm = Mine Mountain, hg = Mercury, cd = Camp Desert Rock, rm = Rainier Mesa, bf = Oak Spring Butte, ts = Topopah Spring, jf = Jackass Flats, and yl = Yucca Lake. For the actual location of these maps, see Appendix II.

Station	Dip Direction	Dip	Slip Angle
jr1	242.	87.	-142.
jr2b	78.	87.	-168.
jr3a	107.	87.	-169.
jr3b	102.	86.	-173.
jr3c	76.	77.	-166.
jr3d	279.	79.	-169.
jr3f	268.	88.	-158.
jr4a	64.	84.	-152.
jr4b	62.	80.	-151.
bf1	90.	87.	-010.
bf2	71.	76.	-101.
pr1a	48.	55.	-052.
pr1b	70.	63.	-072.
pr2a	75.	57.	-077.
pr2b	72.	56.	-078.
pr3	232.	59.	-152.
cs1	150.	81.	-025.
cs2	242.	71.	-049.
cs3	276.	72.	-152.
cs4	333.	49.	-041.
cs5	316.	73.	-054.
cs6	145.	89.	-015.
cs7	313.	50.	-042.
cs6a	297.	80.	-090.
cs6b	309.	66.	-088.
cs6c	311.	87.	-066.
cs6d	315.	84.	-036.
cs6e	315.	89.	-053.
cs7a	320.	88.	-034.
cs7b	228.	82.	-160.
cs7c	45.	57.	-170.
cs8a	280.	83.	-057.
cs8b	255.	81	-045.
cs8c	304.	50.	-019.
cs9a	60.	82.	-120.
cs9b	68.	89.	-128.
cs9c	76.	78.	-126.
cs9d	75.	77.	-124.
cs10a	95.	82.	-140.
cs10b	95.	78.	-122.
cs11a	315.	87.	-051.
cs11b	273.	78.	-170.
cs11c	108.	85.	-045.
cs11d	273.	78.	-061.
cs11e	96.	89.	-129.
cs11f	102.	84.	-142.

cs12a	332.	56.	-049.
cs12b	329.	50.	-035.
cs12c	327.	48.	-056.
cs12d	322.	48.	-064.
cs12e	332.	54.	-063.
cs12f	316.	37.	-055.
cs12g	318.	38.	-069.
cs12h	305.	64.	-072.
cs12i	305.	66.	-071.
cs12j	320.	81.	-023.
cs6f	300.	77.	-080.
cs13a	300.	41.	-072.
cs13b	305.	41.	-074.
cs13c	306.	34.	-082.
cs13d	302.	38.	-090.
cs13e	210.	41.	-143.
cs13f	207.	45.	-145.
cs13g	195.	36.	-158.
cs13h	212.	35.	-137.
cs14a	195.	64.	-012.
cs14b	295.	74.	-061.
cs14c	296.	72.	-060.
cs14d	294.	68.	-070.
cs15a	200.	68.	-146.
cs15b	195.	69.	-155.
cs15c	183.	72.	-130.
cs15d	182.	67.	-132.
cs15e	218.	87.	-130.
cs15f	218.	86.	-135.
cs15g	221.	84.	-135.
cs15h	211.	89.	-135.
cs16a	260.	43.	-115.
cs16b	257.	40.	-104.
cs16c	284.	74.	-121.
cs16d	295.	73.	-118.
cs16e	279.	68.	-104.
cs17a	318.	83.	-077.
cs17b	320.	75.	-063.
cs17c	316.	72.	-069.
cs17d	313.	76.	-070.
cs17e	308.	87.	-064.
cs17f	321.	88.	-086.
cs17g	315.	80.	-045.
cs17h	304.	84.	-063.
cs17i	312.	71.	-072.
cs18a	132.	77.	-002.
cs18b	145.	75.	-175.
pv1	312.	44.	-028.
pv2	200.	88.	-042.
pv3	23.	75.	-138.
pv4a	311.	55.	-077.
pv4b	315.	57.	-082.
pv5a	47.	54.	-063.
pv5b	60.	54.	-159.

sm1	313.	67.	-102.
sm2a	252.	85.	-090.
sm2b	17.	69.	-130.
sm2c	202.	62.	-032.
sm2d	192.	57.	-040.
pv6a	026.	88.	-171.
pv6b	203.	74.	-020.
pv6c	205.	77.	-007.
pv6d	208.	68.	-010.
pv6e	016.	89.	-177.
pv7	150.	72.	-075.
pv8a	100.	69.	-101.
pv8b	96.	64.	-113.
pv8c	270.	65.	-075.
pv9a	126.	67.	-077.
pv9b	117.	71.	-076.
pv9c	118.	71.	-077.
pv10	250.	70.	-070.
pv11a	83.	59.	-027.
pv11b	334.	32.	-114.
pv12a	47.	74.	-068.
pv12b	47.	72.	-085.
pv12c	43.	72.	-095.
pv13a	317.	73.	-101.
pv13b	318.	69.	-100.
pv13c	7.	78.	-134.
pv14a	13.	73.	-021.
pv14b	191.	51.	-059.
pv15	171.	54.	-155.
pv16	322.	66.	-010.
pv17	294.	68.	-102.
pv18	48.	86.	-007.
pv19	180.	78.	-118.
mm1a	281.	66.	-114.
mm1b	281.	56.	-112.
mm1c	259.	73.	-116.
mm1d	270.	67.	-121.
mm1e	346.	86.	-008.
mm1f	273.	15.	-127.
mm1g	270.	29.	-129.
mm2a	142.	72.	-165.
mm2b	148.	67.	-158.
mm2c	148.	75.	-165.
mm2d	123.	53.	-166.
mm2e	122.	82.	-163.
mm2f	131.	90.	-161.
mm3a	118.	68.	-102.
mm3b	198.	42.	-125.
mm3c	193.	34.	-124.
mm3d	311.	58.	-080.
mm3e	309.	60.	-090.
mm4	211.	54.	-120.
mm5a	115.	66.	-043.
mm5b	123.	48.	-053.

mm6	119.	45.	-111.
mm7a	288.	82.	-122.
mm7b	205.	87.	-065.
mm8a	313.	59.	-032.
mm8b	314.	71.	-019.
mm9a	123.	51.	-125.
mm9b	141.	50.	-145.
mm10	13.	37.	-163.
mm11	81.	42.	-106.
hg1a	326.	60.	-177.
hg1b	324.	66.	-165.
hg1c	310.	59.	-177.
hg1d	319.	63.	-171.
hg2a	337.	82.	-006.
hg2b	355.	88.	-005.
hg2c	355.	88.	-177.
hg2d	350.	85.	-175.
hg2e	348.	83.	-174.
hg3a	277.	86.	-100.
hg3b	139.	50.	-084.
hg3c	141.	50.	-088.
hg3d	124.	62.	-107.
hg3e	298.	81.	-118.
hg3f	297.	76.	-120.
hg3g	10.	70.	-100.
hg4a	180.	88.	-000.
hg4b	170.	90.	-006.
hg4c	169.	84.	-165.
hg4d	168.	86.	-000.
hg4e	315.	26.	-032.
hg4f	355.	88.	-022.
hg4g	159.	74.	-168.
hg4h	159.	74.	-167.
cd1	357.	79.	-063.
gqcd1	111.	70.	-055
gqcd2	314.	74.	-124.
gqcs1	354.	70.	-116.
gqjf1	315.	65.	-028.
gqpv1	282.	63.	-102.
gqpv2	079.	60.	-111.
gqrm1	316.	43.	-153.
gqrm2	307.	59.	-170.
gqrm3	290.	58.	-019.
gqts1	250.	64.	-052.
gqyl1	317.	60.	-139.

APPENDIX II

Following is a listing of the U.S.G.S. maps used to compile Plate I. The diagram that follows is of the location of the various maps with respect to the borders of the Nevada Test Site.

Barnes, Harley, R. L. Christiansen, and F. M. Byers, Jr., Geologic map of the Jangle Ridge quadrangle, Nye and Lincoln Counties, Nevada, *U.S. Geol. Surv. Geol. Quad. Map GQ-373*, 1965.

Barnes, Harley, E. B. Ekren, C. L. Rogers, and D. L. Hedlund, Geologic and tectonic map of the Mercury quadrangle, Nyee and Clark Counties, Nevada, *U.S. Geol. Surv. Misc. Inv. Map I-1197*, 1982.

Barnes, Harley, F. N. Houser, and F. G. Poole, Geology of the Oak Spring quadrangle, Nye County, Nevada, *U.S. Geol. Surv. Geol. Quad. Map GQ-214*, 1963.

Byers, F. M., Jr. and Harley Barnes, Geologic map of the Paiute Ridge quadrangle, Nye and Lincoln Counties, Nevada, *U.S. Geol. Surv. Geol. Quad. Map GQ-577*, 1967.

Byers, F. M., Jr., W. J. Carr, R. L. Christiansen, P. W. Lipman, P. P. Orkild, and W. D. Quinlivan, Geologic map of the Timber Mountain caldera area, Nye County, Nevada, *U.S. Geol. Surv. Misc. Geol. Inv. Map I-891*, 1976.

Byers, F. M., Jr., C. L. Rogers, W. J. Carr, and S. J. Luft, Geologic map of the Buckboard Mesa quadrangle, Nye County, Nevada, *U.S. Geol. Surv. Geol. Quad. Map GQ-552*, 1966.

Carr, W. J. and W. D. Quinlivan, Geologic map of the Timber Mountain quadrangle, Nye County, Nevada, *U.S. Geol. Surv. Geol. Quad. Map GQ-503*, 1966.

Christiansen, R. L. and P. W. Lipman, Geologic map of the Topopah Spring NW quadrangle, Nye County, Nevada, *U.S. Geol. Surv. Geol. Quad. Map GQ-444*, 1965.

Christiansen, R. L. and D. C. Noble, Geologic map of the Trail Ridge quadrangle, Nye County, Nevada, *U.S. Geol. Surv. Geol. Quad. Map GQ-774*, 1968.

Colton, R. B. and E. J. McKay, Geologic map of the Yucca Flat quadrangle, Nye County, Nevada, *U.S. Geol. Surv. Geol. Quad. Map GQ-582*, 1966.

Cornwall, H. R. and F. J. Kleinhampl, Geology of the Bare Mountain quadrangle, Nye County, Nevada, *U.S. Geol. Surv. Geol. Quad. Map GQ-157*, 1961.

Ekren, E. B., R. E. Anderson, P. P. Orkild, and E. N. Hinrichs, Geologic map of the Silent Butte quadrangle, Nye County, Nevada, *U.S. Geol. Surv. Geol. Quad. Map GQ-493*, 1966.

Ekren, E. B. and K. A. Sargent, Geologic map of the Skull Mountain quadrangle, Nye County, Nevada, *U.S. Geol. Surv. Geol. Quad. Map GQ-387*, 1965.

Gibbons, A. B., E. N. Hinrichs, W. R. Hansen, and R. W. Lemke, Geology of the Rainier Mesa quadrangle, Nye County, Nevada, *U.S. Geol. Surv. Geol. Quad. Map GQ-215*, 1963.

Hinrichs, E. N., Geologic map of the Camp Desert Rock quadrangle, Nye County, Nevada, *U.S. Geol. Surv. Geol. Quad. Map GQ-726*, 1968.

Hinrichs, E. N., R. D. Krushensky, and S. J. Luft, Geologic map of the Ammonia Tanks quadrangle, Nye County, Nevada, *U.S. Geol. Surv. Geol. Quad. Map GQ-638*, 1967.

Hinrichs, E. N. and E. J. McKay, Geologic map of the Plutonium Valley quadrangle, Nye and Lincoln Counties, Nevada, *U.S. Geol. Surv. Geol. Quad. Map GQ-384*, 1965.

Houser, F. N. and F. G. Poole, Preliminary geologic map of the Climax stock and vicinity, Nye County, Nevada, *U.S. Geol. Surv. Misc. Geol. Inv. Map I-328*, 1960.

Lipman, P. W. and E. J. McKay, Geologic map of the Topopah Spring SW quadrangle, Nye County, Nevada, *U.S. Geol. Surv. Geol. Quad. Map GQ-439*, 1965.

Lipman, P. W., Quinlivan, W. D., W. J. Carr, and R. E. Anderson, Geologic map of the Thirsty Canyon SE quadrangle, Nye County, Nevada, *U.S. Geol. Surv. Geol. Quad. Map GQ-489*, 1966.

McKay, E. J. and K. A. Sargent, Geologic map of the Lathrop Wells quadrangle, Nye County, Nevada, *U.S. Geol. Surv. Geol. Quad. Map GQ-883*, 1970.

McKay, E. J. and W. P. Williams, Geology of the Jackass Flats quadrangle, Nye County, Nevada, *U.S. Geol. Surv. Geol. Quad. Map GQ-368*, 1964.

McKeown, F. A., Geologic map of the Yucca Lake quadrangle, Nye County, Nevada, *U.S. Geol. Surv. Geol. Quad. Map GQ-1327*, 1976.

Noble, D. C., R. D. Krushensky, E. J. McKay, and J. R. Ege, Geologic map of the Dead Horse Flat quadrangle, Nye County, Nevada, *U.S. Geol. Surv. Geol. Quad. Map GQ-614*, 1967.

O'Connor, J. T., R. E. Anderson, and P. W. Lipman, Geologic map of the Thirsty Canyon quadrangle, Nye County, Nevada, *U.S. Geol. Surv. Geol. Quad. Map GQ-524*, 1966.

Orkild, P. P., Geology of the Tippipah Spring quadrangle, Nye County, Nevada, *U.S. Geol. Surv. Geol. Quad. Map GQ-213*, 1963.

Orkild, P. P., Geologic map of the Mine Mountain quadrangle, Nye County, Nevada, *U.S. Geol. Surv. Geol. Quad. Map GQ-746*, 1968.

Orkild, P. P. and J. T. O'Connor, Geologic map of the Topopah Spring quadrangle, Nye County, Nevada, *U.S. Geol. Surv. Geol. Quad. Map GQ-849*, 1970.

Poole, F. G., Geologic map of the Frenchman Flat quadrangle, Nye, Lincoln, and Clark Counties, Nevada, *U.S. Geol. Surv. Geol. Quad. Map GQ-456*, 1965.

Poole, F. G., D. P. Elston, and W. J. Carr, Geologic map of the Cane Spring quadrangle, Nye County, Nevada, *U.S. Geol. Surv. Geol. Quad. Map GQ-455*, 1965.

Rogers, C. L. and D. C. Noble, Geologic map of the Oak Spring Butte quadrangle, Nye County, Nevada, *U.S. Geol. Surv. Geol. Quad. Map GQ-822*, 1969.

Sargent, K. A., S. J. Luft, A. B. Gibbons, and D. L. Hoover, Geologic map of the Quartet Dome quadrangle, Nye County, Nevada, *U.S. Geol. Surv. Geol. Quad. Map GQ-496*, 1966.

Sargent, K. A., E. J. McKay, and B. C. Burchfiel, Geologic map of the Striped Hills quadrangle, Nye County, Nevada, *U.S. Geol. Surv. Geol. Quad. Map GQ-882*, 1970.

Sargent, K. A. and J. H. Stewart, Geologic map of the Specter Range NW quadrangle, Nye County, Nevada, *U.S. Geol. Surv. Geol. Quad. Map GQ-884*, 1971.

Map showing quadrangle locations in the Nevada Test Site region, including Pahute Mesa (I-367), Wheelbarrow Peak-Rainier Mesa (I-754), Trail Ridge (60-774), Silent Butte (60-493), Dead Horse Flat (60-614), Quartet Dome (60-495), Oak Spring Butte (60-622), Thirsty Canyon (60-524), Scrugham Peak (60-693), Ammonia Tanks (60-632), Rainier Mesa (60-215), Oak Spring (60-214), Jangle Ridge (60-553), Timber Mountain (60-503), Buckboard Mesa (60-552), Tippipah Spring (60-213), Yucca Flat (60-562), Paiute Ridge (60-577), Yucca Flat (I-550), Timber Mountain (I-651), Topopah Spring NW (60-444), Topopah Spring (60-549), Mine Mountain (60-746), Yucca Lake (60-1327), Plutonium Valley (60-384), Topopah Spring SW (60-439), Jackass Flats (60-383), Skull Mountain (60-387), Cane Spring (60-433), Frenchman Flat (60-434), Lathrop Wells (60-682), Striped Hills (60-682), Specter Range NW (60-684), Camp Desert Rock (60-728), Mercury, and Lathrop Wells.